

# pH-dependent random coil $^1\text{H}$ , $^{13}\text{C}$ , and $^{15}\text{N}$ chemical shifts of the ionizable amino acids: a guide for protein $\text{p}K_{\text{a}}$ measurements

Gerald Platzer · Mark Okon · Lawrence P. McIntosh

Received: 29 July 2014 / Accepted: 9 September 2014  
© Springer Science+Business Media Dordrecht 2014

**Abstract** The  $\text{p}K_{\text{a}}$  values and charge states of ionizable residues in polypeptides and proteins are frequently determined via NMR-monitored pH titrations. To aid the interpretation of the resulting titration data, we have measured the pH-dependent chemical shifts of nearly all the  $^1\text{H}$ ,  $^{13}\text{C}$ , and  $^{15}\text{N}$  nuclei in the seven common ionizable amino acids ( $X = \text{Asp, Glu, His, Cys, Tyr, Lys, and Arg}$ ) within the context of a blocked tripeptide, acetyl-Gly- $X$ -Gly-amide. Alanine amide and  $N$ -acetyl alanine were used as models of the N- and C-termini, respectively. Together, this study provides an essentially complete set of pH-dependent intra-residue and nearest-neighbor reference chemical shifts to help guide protein  $\text{p}K_{\text{a}}$  measurements. These data should also facilitate pH-dependent corrections in algorithms used to predict the chemical shifts of random

coil polypeptides. In parallel, deuterium isotope shifts for the side chain  $^{15}\text{N}$  nuclei of His, Lys, and Arg in their positively-charged and neutral states were also measured. Along with previously published results for Asp, Glu, Cys, and Tyr, these deuterium isotope shifts can provide complementary experimental evidence for defining the ionization states of protein residues.

**Keywords** Protein electrostatics · pH titration · Chemical shift · Scalar coupling · Deuterium isotope shift · Hydrogen exchange

## Introduction

Electrostatic interactions are central to the structures, dynamics, and functions of proteins (Creighton 2010). These interactions are established in large part by the pH-dependent protonation states of their termini and ionizable side chains. Although substantial progress has been made in theoretical methods to predict the charges and acid dissociation equilibrium constants ( $\text{p}K_{\text{a}}$  values) of these moieties within the context of a folded protein (Alexov et al. 2011; Nielsen et al. 2011), experimental measurements remain critical. This is particularly true for functionally important residues, which often have significantly perturbed  $\text{p}K_{\text{a}}$  values (Forsyth et al. 2002; Harris and Turner 2002) and may be involved in complex, coupled ionization equilibria (Forman-Kay et al. 1992; Lindman et al. 2006; Ludwiczek et al. 2013). Crystallographically- and NMR spectroscopically-determined structures are invaluable for understanding protein electrostatics. However, in the absence of neutron (Blakeley et al. 2008; Niimura and Bau 2008) or very high-resolution X-ray diffraction data (Lecomte et al. 2008), the protonation

**Electronic supplementary material** The online version of this article (doi:10.1007/s10858-014-9862-y) contains supplementary material, which is available to authorized users.

G. Platzer · M. Okon · L. P. McIntosh (✉)  
Department of Biochemistry and Molecular Biology, Life Sciences Centre, 2350 Health Sciences Mall, University of British Columbia, Vancouver, BC V6T 1Z3, Canada  
e-mail: mcintosh@chem.ubc.ca

G. Platzer · M. Okon · L. P. McIntosh  
Department of Chemistry, University of British Columbia, Vancouver, BC V6T 1Z1, Canada

G. Platzer · M. Okon · L. P. McIntosh  
Michael Smith Laboratories, University of British Columbia, Vancouver, BC V6T 1Z4, Canada

### Present Address:

G. Platzer  
Department of Structural and Computational Biology, Max F. Perutz Laboratories, University of Vienna, Vienna Biocenter Campus 5, 1030 Vienna, Austria

states of residues in these structures are often experimentally undefined and thus inferred from physicochemical arguments. In favorable cases, the ionization states and  $pK_a$  values associated with selected side chains can be determined using approaches spanning potentiometry (Parsons and Rafferty 1972) to pH-dependent stability (Fitch et al. 2002), chemical reactivity (Tolbert et al. 2005), and enzymatic measurements (Knowles 1976). Given suitable chromophores/fluorophores, various forms of absorption/emission spectroscopy can also be used. Of all such experimental methods, NMR spectroscopy is the most powerful technique for investigating the residue-specific charge states and  $pK_a$  values of proteins and their complexes.

The observation of the  $^1\text{H}$ -NMR signal(s) from the acidic proton(s) of an ionizable functional group provides unambiguous evidence that it is indeed protonated. However, labile nitrogen-, oxygen- and sulfur-bonded protons typically exchange rapidly with those of water (Englander and Kallenbach 1983; Wüthrich and Wagner 1979). Thus, their direct detection usually requires conditions of low temperature, pH, and general acid/base buffer concentrations (Liepinsh and Otting 1996; Liepinsh et al. 1992), combined with pulse sequences that minimally perturb water magnetization (Gueron et al. 1991; Zheng and Price 2010). Even so, observable acidic protons also tend to be protected from exchange (HX) by hydrogen bonding and burial within the interior of a protein or protein complex. As a result of such structure-specific environments, the associated residues often have perturbed  $pK_a$  values and their acidic protons may resonate over a wide range of chemical shifts relative to those found for model reference compounds. This is advantageous for simple  $^1\text{H}$ -NMR measurements if yielding well resolved signals downfield of  $\sim 10$  ppm (Baturin et al. 2011; Schubert et al. 2007). However, labile protons with less perturbed chemical shifts may remain undetected by one-dimensional (1D)  $^1\text{H}$ -NMR approaches due to spectral overlap within the envelope of water and protein signals, and by conventional 2D  $^{15}\text{N}/^{13}\text{C}$  heteronuclear correlation experiments due to their optimization for amides and aromatic/aliphatic groups, respectively.

When properly optimized, acidic protons on arginine, histidine and lysine side chains, as well as the N-terminal amine, can often be detected in a  $^{15}\text{N}$ -HSQC or -HMQC spectrum due to a strong one-bond  $^1J_{\text{NH}}$  coupling to the directly attached  $^{15}\text{N}$  (provided that the HX rate constant  $k_{\text{ex}} < ^1J_{\text{NH}}$  to allow coherence transfer (Henry and Sykes 1990; Segawa et al. 2008)). These functional groups are easily recognized by their diagnostic  $^{15}\text{N}$  shifts, which are clearly resolved from those of the protein amides and indoles (Blomberg et al. 1976; Blomberg and Rüterjans 1983; Cohen et al. 1983). In addition, the number of slowly exchanging protons on the  $^{15}\text{N}$  can be determined unambiguously from

$^1J_{\text{NH}}$  multiplet patterns in spectra recorded without  $^1\text{H}$  decoupling in the indirect dimension. This is particularly helpful for distinguishing  $-\text{NH}_3^+$  versus  $-\text{NH}_2$  groups (Poon et al. 2006; Takayama et al. 2008a, b). In contrast, oxygen- and sulfur-bonded protons lack such useful one-bond couplings. Thus, direct detection of these protons requires the use of less sensitive homo- or heteronuclear multiple-bond scalar correlation experiments or potentially ambiguous NOE approaches (Baturin et al. 2011; Liepinsh et al. 1992; Nordstrand et al. 1999). Alternatively, oxygen- and sulfur-bonded protons may be observed in 1D  $^1\text{H}$ -NMR spectra recorded while filtering against protons directly bonded to  $^{13}\text{C}$  and  $^{15}\text{N}$  nuclei in a protein uniformly labeled with these two isotopes (Brockerman et al. 2014). In the event that an acidic proton cannot be observed directly because of rapid HX or because of spectral overlap that cannot be resolved using scalar or NOE correlations, its presence may still be revealed through deuterium isotope shift measurements (Hansen 2000, 2007; Ladner et al. 1975; Led and Petersen 1979; Takeda et al. 2009, 2010, 2014; Tugarinov 2014; Wang et al. 1996).

The  $pK_a$  values and hence protonation states of ionizable residues in proteins are most frequently determined via NMR-monitored pH titrations. Over the course of the titration, one generally measures the signals from selected non-exchangeable  $^1\text{H}$ ,  $^{13}\text{C}$  or  $^{15}\text{N}$  nuclei within a given residue, whose chemical shifts (or scalar couplings) are *assumed* to report the protonation state of that residue. Fitting the chemical shift versus pH data to a suitable equation for a chemical equilibrium in the fast exchange limit yields the apparent  $pK_a$  values governing the observed titrations (McIntosh et al. 2011). However, a titration curve may deviate from that expected for a simple acid/base equilibrium as reflected by the familiar Hendersen-Hasselbalch equation. This phenomenon can arise from coupled protonation equilibria, such that a residue exhibits multiple microscopic  $pK_a$  values that depend upon the exact charge states of all other interacting residues (McIntosh et al. 2011; Rabenstein and Sayer 1976b; Shrager et al. 1972; Søndergaard et al. 2008; Surprenant et al. 1980; Szakacs et al. 2004; Ullmann 2003). Chemical shift perturbations may also result from other pH-dependent effects, including changes in the electric field around a nucleus due to the deprotonation of neighboring residues (Buckingham 1960; Kukic et al. 2013), as well as local or global protein conformational transitions (Tomlinson et al. 2010; Wishart 2011). Indeed, it is important to stress that, for most nuclei in a protein, the range of possible chemical shift changes induced upon folding or ligand binding encompass those due to (de)protonation (Ulrich et al. 2008). Thus, caution must be exercised when trying to infer the charge state of a residue solely from the chemical shifts of its  $^{13}\text{C}$ ,  $^{15}\text{N}$ , or non-exchangeable  $^1\text{H}$  nuclei.

With these caveats in mind, the  $pK_a$  value(s) of an ionizable residue is most confidently determined when several nuclei in that residue (particularly if part of the acidic/basic functional group) report co-incident titrations and exhibit chemical shift changes comparable in magnitude and sign (i.e., upfield or downfield) to those shown by reference random coil polypeptides. Most of these reference values can be found in papers from the pioneering days of biological NMR spectroscopy (Batchelor et al. 1975; Blomberg et al. 1976, 1977; Blomberg and Rüterjans 1983; Bundi and Wüthrich 1979a, b; Cohen et al. 1983; Freedman et al. 1973; Howarth and Lilley 1978; Kanamori et al. 1978, Keim et al. 1973, 1974; London 1980; London et al. 1977, 1978; Quirt et al. 1974; Rabenstein and Sayer 1976a; Richarz and Wüthrich 1978; Surprenant et al. 1980). However, these studies were carried out with a variety of amino acid derivatives, polypeptides, or proteins under a range of experimental conditions and, to add potential confusion, were reported using several different chemical shift referencing protocols. Accordingly, we have measured the pH-dependent chemical shifts of essentially all the  $^1\text{H}$ ,  $^{13}\text{C}$ , and  $^{15}\text{N}$  nuclei in the seven common ionizable amino acids within the context of a blocked tripeptide. The few missing values correspond to rapidly exchanging protons not detected under alkaline conditions. Alanine derivatives were used as models of the N- and C-termini. Deuterium isotope shifts for the side chain  $^{15}\text{N}$  nuclei of His, Lys, and Arg in their cationic and neutral states were also determined. Collectively, this provides an almost complete set of intra-residue and nearest-neighbor reference  $^1\text{H}$ ,  $^{13}\text{C}$ , and  $^{15}\text{N}$  chemical shift data to guide  $pK_a$  measurements and to aid in interpreting the NMR-monitored pH titrations of polypeptides and proteins. These data should also better enable pH-dependent corrections in algorithms used to predict the chemical shifts of random coil polypeptides (Wishart 2011).

## Materials and methods

### Samples

*N*-acetyl alanine (CAS 97-69-8) and alanine amide (CAS 33208-99-0) were obtained from Chem-Impex. A series of acetyl-Gly-X-Gly-amide (X = Asp, Glu, His, Cys, Tyr, Lys, and Arg) tripeptides were purchased from Biometik (HPLC purified to >95 %). Uniformly  $^{13}\text{C}_6/^{15}\text{N}_4$ -enriched L-arginine was bought from Sigma-Aldrich.

### NMR spectroscopy

The tripeptides and alanine derivatives were prepared at ~10 mM in 50 mM NaCl and 5 %  $\text{D}_2\text{O}$  ( $D = ^2\text{H}$ ). DSS

(4,4-dimethyl-4-silapentane-1-sulfonic acid; 1 mM) was included as a pH-independent internal reference (Demarco 1977; Wishart 2011). For the cysteine tripeptide, 10 mM TCEP (tris(2-carboxyethyl)phosphine) was also present as a reductant. Sample pH values were measured at room temperature (~20 °C) using a Thermal Scientific Orion\* 3-Star pH meter with an Orion ROSS micro pH electrode (8220BNWP), and adjusted by addition of HCl or NaOH (0.1 or 1 M) in small aliquots. Spectra were recorded at 25 °C using Bruker Avance III 500 and 600 MHz spectrometers with TCI CryoProbes. The  $^1\text{H}$  and  $^{13}\text{C}$  signals were referenced directly to the internal DSS, and the  $^{15}\text{N}$  referenced indirectly via magnetogyric ratios (Wishart 2011). Chemical shifts were measured using 1D  $^1\text{H}$ -NMR along with 2D  $^{13}\text{C}$ -HSQC spectra for protonated carbons, multiple-bond  $^{13}\text{C}$ -HMBC spectra for non-protonated carbons,  $^{15}\text{N}$ -HSQC spectra for slowly exchanging protonated nitrogens, and multiple-bond  $^{15}\text{N}$ -HMBC spectra for deprotonated or rapidly exchanging protonated nitrogens. For the latter, samples were in 99 %  $\text{D}_2\text{O}$  to minimize signal loss due to HX, and the reported chemical shifts were corrected for deuterium isotope shifts. The isotope shifts were determined by comparing spectra recorded in 95 %  $\text{H}_2\text{O}$  versus 99 %  $\text{D}_2\text{O}$  solutions under similar pH (or pH\*) conditions such that the functional group in question was effectively fully charged or neutral. Here, pH\* denotes the uncorrected pH meter reading (Krezel and Bal 2004).

The  $^{13}\text{C}_6/^{15}\text{N}_4$ -L-arginine was initially 10 or 100 mM in 50 mM NaCl with 1 mM DSS and 5 %  $\text{D}_2\text{O}$ , and the sample pH increased using small aliquots of 0.1 or 1 M KOH. To obtain pH > 13, solid KOH was added directly to the solution. For measurements under very alkaline conditions, KOH is preferable over NaOH to minimize electrode errors (Licht 1985; Popov et al. 2006). Samples were in 5 mm NMR tubes, except under very high pH conditions, where a 3 mm tube was used to allow tuning at the resulting elevated ionic strength. Chemical shifts were measured from 1D  $^{13}\text{C}$ -decoupled  $^1\text{H}$ -NMR,  $^1\text{H}/^{15}\text{N}$ -decoupled  $^{13}\text{C}$ -NMR (with  $^1\text{H}$ -NOE), and  $^1\text{H}/^{13}\text{C}$ -decoupled  $^{15}\text{N}$ -NMR (with  $^1\text{H}$ -NOE) spectra. The TCI Cryo-Probe is designed for direct detection of  $^1\text{H}$  and  $^{13}\text{C}$ , but not  $^{15}\text{N}$ , and thus a 100 mM sample of  $^{13}\text{C}_6/^{15}\text{N}_4$ -arginine was required for the latter  $^{15}\text{N}$ -NMR measurements.

### Data analysis

Spectra were processed using Topspin 3. The pH-dependent  $^1\text{H}$ ,  $^{13}\text{C}$ , or  $^{15}\text{N}$  chemical shifts were fit separately with KaleidaGraph or GraphPad Prism to standard equations for one, or in the case of arginine, two sequential titrations in order to obtain  $pK_a$  and limiting chemical shift values (McIntosh et al. 2011). These values also include possible effects of increasing ionic strength over the course of the



**Fig. 1** pH-dependent chemical shift changes ( $\Delta\delta$  in ppm; negative is upfield) upon *deprotonation* of the ionizable amino acid functional groups (atoms and  $\Delta\delta$  values are colored as: acidic proton, *red*; oxygens and non-labile protons, *black* within the named residue and *grey* in flanking blocked glycines; carbon, *green*; nitrogen, *blue*; sulfur, *yellow*; phosphate, *magenta*). The data are from Table 1 and Supplemental Table S1, or in the case of the phosphoamino acid peptides (second ionization step), from (Bienkiewicz and Lumb 1999). Data for  $^{13}\text{C}/^{15}\text{N}$ -L-arginine are due to deprotonation of the guanidinium moiety in the context of fully deprotonated amino ( $pK_a$  9.15) and carboxyl groups (Table 1 and Supplemental Table S2). Values for the neutral forms of the Gly-His-Gly tripeptide and arginine are tautomer averaged

titrations due to the addition of acid or base. As expected with only a single ionizable group in the alanine derivatives and blocked tripeptides, all constituent nuclei exhibited coincident titrations. Thus, the cited  $pK_a$  values, with estimated errors of  $\pm 0.05$  units due to pH measurements, are the average of the very similar fit values for each nucleus showing a substantial pH-dependent chemical shift change. These averaged  $pK_a$  values agree closely with those reported previously for the termini and Asp, Glu, His, Cys, Tyr, and Lys side chains in alanine pentapeptides (Grimsley et al. 2009). Analysis of the titration curves also yielded plateau chemical shift values for the tripeptides and arginine in their fully protonated and deprotonated forms, with fitting errors of  $\pm 0.02$  ppm for  $^1\text{H}$  nuclei,  $\pm 0.08$  ppm for  $^{13}\text{C}$ , and  $\pm 0.06$  ppm for  $^{15}\text{N}$ . These chemical shift data have been deposited in the BioMagResBank (Ulrich et al. 2008).

## Results

The pH-dependent chemical shifts of the ionizable amino acids were measured in the context of a blocked tripeptide, acetyl-Gly-X-Gly-amide. Along with parallel studies of *N*-acetyl alanine and alanine amide, this provides a near complete database of the conformationally-averaged intra-residue and nearest-neighbor  $^1\text{H}$ ,  $^{13}\text{C}$ , and  $^{15}\text{N}$  chemical shift changes resulting from the deprotonation of terminal and side chain groups. These results are summarized in Fig. 1 and Table 1 (with complete data sets in Supplemental Tables S1 and S2), and discussed below. A review of key literature and/or representative studies on each amino acid type is also

**Table 1** pH-dependent chemical shifts (ppm) of the ionizable amino acids <sup>a</sup>

Nucleus type	Nucleus	$\delta$ (HA)	$\delta$ (A)	$\Delta\delta$ (A-HA)
<i>N-terminal amine: alanine-amide (<math>pK_a</math> 8.23)</i>				
$^1\text{H}$	H (amine)	8.04		
	H $\alpha$	4.10	3.51	-0.59
	H $\beta$ (methyl)	1.54	1.27	-0.27
$^{13}\text{C}$	C $\alpha$	51.7	52.7	1.0
	C $\beta$ (methyl)	19.3	22.9	3.6
	CO	176.0	184.6	8.5
$^{15}\text{N}$	N (amine)	40.4	33.8	-6.6
<i>C-terminal carboxylic acid: N-acetyl alanine (<math>pK_a</math> 3.55)</i>				
$^1\text{H}$	HN	8.35	7.94	-0.41
	H $\alpha$	4.33	4.12	-0.21
	H $\beta$ (methyl)	1.41	1.32	-0.09
$^{13}\text{C}$	C $\alpha$	51.4	53.7	2.3
	C $\beta$ (methyl)	18.8	20.1	1.3
	CO	179.6	183.0	3.4
$^{15}\text{N}$	N	110.5	115.7	5.2
<i>Aspartic acid: Ac-Gly-Asp-Gly-NH<sub>2</sub> (<math>pK_a</math> 3.86)</i>				
$^1\text{H}$	HN	8.55	8.38	-0.17
	H $\alpha$	4.78	4.61	-0.17
	H $\beta$ (avg.)	2.93	2.70	-0.23
	H $\delta$ 2 (carboxyl)	>10		
$^{13}\text{C}$	C $\alpha$	52.9	54.3	1.4
	C $\beta$	38.0	41.1	3.0
	C $\gamma$ (carboxyl)	177.1	180.3	3.2
	CO	175.8	176.9	1.1
$^{15}\text{N}$	N	118.7	120.2	1.5
<i>Glutamic acid: Ac-Gly-Glu-Gly-NH<sub>2</sub> (<math>pK_a</math> 4.34)</i>				
$^1\text{H}$	HN	8.45	8.57	0.12
	H $\alpha$	4.39	4.29	-0.10
	H $\beta$ (avg.)	2.08	2.02	-0.06
	H $\gamma$	2.49	2.27	-0.22
	H $\epsilon$ 2 (carboxyl)	>10		
$^{13}\text{C}$	C $\alpha$	56.0	56.9	1.0
	C $\beta$	28.5	30.0	1.5
	C $\gamma$	32.7	36.1	3.5
	C $\delta$ (carboxyl)	179.7	183.8	4.1
	CO	176.5	177.0	0.6
$^{15}\text{N}$	N	119.9	120.9	1.0

**Table 1** continued

Nucleus type	Nucleus	$\delta$ (HA)	$\delta$ (A)	$\Delta\delta$ (A–HA)
<i>Histidine: Ac-Gly-His-Gly-NH<sub>2</sub> (pK<sub>a</sub> 6.45)<sup>c</sup></i>				
<sup>1</sup> H	HN	8.55	~8.35 <sup>d</sup>	~−0.2
	H $\alpha$	~4.75 <sup>d</sup>	4.59	~−0.2
	H $\beta$ (avg.)	3.25	3.08	−0.17
	H $\delta$ 2	7.30	6.97	−0.33
	H $\epsilon$ 1	8.60	7.68	−0.92
	H $\delta$ 1	>10		
	H $\epsilon$ 2	>10		
<sup>13</sup> C	C $\alpha$	55.1	56.7	1.6
	C $\beta$	28.9	31.3	2.4
	C $\gamma$	131.0	135.3	4.2
	C $\delta$ 2	120.3	120.0	−0.3
	C $\epsilon$ 1	136.6	139.2	2.6
	CO	174.8	176.2	1.5
	<sup>15</sup> N	N	117.9	119.7 <sup>b</sup>
N $\delta$ 1		175.8	231.3 <sup>b</sup>	56
N $\epsilon$ 2		173.1	181.1 <sup>b</sup>	8
<i>Cysteine: Ac-Gly-Cys-Gly-NH<sub>2</sub> (pK<sub>a</sub> 8.49)</i>				
<sup>1</sup> H	HN	8.48		
	H $\alpha$	4.56	4.28	−0.28
	H $\beta$ (avg.)	2.97	2.88	−0.09
	H $\gamma$ (thiol)	~2.0 <sup>e</sup>		
<sup>13</sup> C	C $\alpha$	58.5	60.6	2.1
	C $\beta$	28.0	29.7	1.7
	CO	175.0	176.9	1.9
<sup>15</sup> N	N	118.7	122.2 <sup>b</sup>	3.6
<i>Tyrosine: Ac-Gly-Tyr-Gly-NH<sub>2</sub> (pK<sub>a</sub> 9.76)</i>				
<sup>1</sup> H	HN	8.16		
	H $\alpha$	4.55	4.49	−0.06
	H $\beta$ (avg.)	3.02	2.94	−0.08
	H $\delta$	7.14	6.97	−0.17
	H $\epsilon$	6.85	6.57	−0.28
	H $\eta$ (phenol)	~9.3 <sup>e</sup>		
	<sup>13</sup> C	C $\alpha$	58.0	58.2
C $\beta$		38.6	38.7	0.1
C $\gamma$		130.5	123.8	−6.7
C $\delta$		133.3	133.2	−0.1
C $\epsilon$		118.4	121.7	3.3
C $\zeta$		157.0	167.4	10.4
CO		176.3	176.7	0.4
<sup>15</sup> N	N	120.1	120.7 <sup>b</sup>	0.6
<i>Lysine: Ac-Gly-Lys-Gly-NH<sub>2</sub> (pK<sub>a</sub> 10.34)</i>				
<sup>1</sup> H	HN	8.40		
	H $\alpha$	4.34	4.30	−0.04
	H $\beta$ (avg.)	1.82	1.78	−0.04
	H $\gamma$	1.44	1.36	−0.08
	H $\delta$	1.68	1.44	−0.24

**Table 1** continued

Nucleus type	Nucleus	$\delta$ (HA)	$\delta$ (A)	$\Delta\delta$ (A–HA)
<sup>1</sup> H	H $\epsilon$	3.00	2.60	−0.40
	H $\zeta$ (amine)	7.52	~1–2 <sup>f</sup>	
<sup>13</sup> C	C $\alpha$	56.4	56.9	0.4
	C $\beta$	32.8	33.2	0.3
	C $\gamma$	24.7	25.0	0.4
	C $\delta$	28.9	33.9	5.0
	C $\epsilon$	42.1	43.1	1.0
	CO	177.0	177.5	0.5
	<sup>15</sup> N	N	121.0	121.7 <sup>b</sup>
N $\zeta$ (amine)		32.7	~25.2 <sup>g</sup>	~−7.5 <sup>g</sup>
<i>Arginine: <sup>13</sup>C/<sup>15</sup>N<sub>4</sub>-Arg (pK<sub>a</sub> 13.9)<sup>h</sup></i>				
<sup>1</sup> H	HN (amine)	7.81		
	H $\alpha$	3.26	3.19	−0.07
	H $\beta$ (avg.)	1.60		< 1–0.11
	H $\gamma$	1.60		< 1–0.11
	H $\delta$	3.19	3.00	−0.19
	H $\epsilon$ (guan.)	7.22		
	H $\eta$ (guan.)	6.67		
<sup>13</sup> C	C $\alpha$	58.4	58.6	0.2
	C $\beta$	34.4	35.2	0.9
	C $\gamma$	27.2	28.1	1.0
	C $\delta$	43.8	44.3	0.5
	C $\zeta$ (guan.)	159.6	163.5	4.0
	CO	185.8	186.1	0.2
	<sup>15</sup> N	N	33.2	33.6
N $\epsilon$ (guan.)		85.6	91.5	5.9
N $\eta$ (guan.)		71.2	93.2	22

<sup>a</sup> Recorded at 25 °C with 50 mM NaCl and 5 % D<sub>2</sub>O, unless indicated. Reported are the fit pK<sub>a</sub> values and end point chemical shifts  $\delta$  (ppm) of the of the acid (HA) and conjugate base (A) forms, along with the chemical shift change upon deprotonation ( $\Delta\delta$ ; negative is upfield). The estimated errors are  $\pm 0.05$  for pK<sub>a</sub> values ( $\pm 0.1$  for arginine),  $\pm 0.02$  ppm for <sup>1</sup>H nuclei,  $\pm 0.08$  ppm for <sup>13</sup>C, and  $\pm 0.06$  ppm for <sup>15</sup>N. Blank values indicate not determined. Prochiral <sup>1</sup>H $\beta$  shifts are averaged. Supplemental Table S1 provides data for the flanking blocked glycines

<sup>b</sup> Recorded in 99 % D<sub>2</sub>O and corrected for the deuterium isotope shift

<sup>c</sup> Data for neutral histidine are an average of ~80 % N<sup>ε2</sup>H and ~20 % N<sup>δ1</sup>H tautomers

<sup>d</sup> Estimated from (Kjaergaard et al. 2011)

<sup>e</sup> From the BioMagResBank (Ulrich et al. 2008)

<sup>f</sup> From (Takayama et al. 2008a)

<sup>g</sup> From (Andre et al. 2007)

<sup>h</sup> Tabulated are the fit chemical shifts for the titration of the guanidinium moiety in <sup>13</sup>C/<sup>15</sup>N<sub>4</sub>-L-arginine with its  $\alpha$ -carboxyl and  $\alpha$ -amine deprotonated (with the exception of the nitrogen-bonded <sup>1</sup>H at pH ~7). Supplemental Table S2 provides full data including the  $\alpha$ -amine titration. Due to bond rotations, the two <sup>15</sup>N<sup>n</sup> and four <sup>1</sup>H<sup>n</sup> each yield one broad signal. The shifts for neutral arginine are tautomer averaged

given. For consistency, titrations are described in terms of increasing pH and thus deprotonation of the acid species to form its conjugate Brønsted-Lowry base.

#### N-terminal amine

Alanine amide was used as a simple model of an N-terminal residue, yielding a  $pK_a$  value of 8.23. The  $\alpha$ -amino  $^{15}\text{N}$  shifts by  $-6.6$  ppm (i.e., upfield) upon deprotonation, and thus serves as an obvious reporter nucleus for measuring the  $pK_a$  value of the N-terminus of a protein. Furthermore, the protonated nitrogen has a relatively unique chemical shift ( $\sim 40$  ppm), distinct from that of the lysine side chain  $^{15}\text{N}^\epsilon$  ( $\sim 33$  ppm), thus potentially allowing its observation as a well-resolved signal in a 1D  $^{15}\text{N}$ -NMR spectrum (Mcintosh et al. 1990; Smith et al. 1987; Zhu et al. 1995). However, detecting the  $^{15}\text{N}$  nucleus indirectly via a 2D  $\text{H}^\alpha(\text{C}^\alpha)\text{N}$ -type experiment recorded with a selectively or uniformly  $^{13}\text{C}/^{15}\text{N}$ -labeled protein should provide improved sensitivity (Andre et al. 2007). Alternatively, the  $^1\text{H}^\alpha$ ,  $^1\text{H}^\beta$ ,  $^{13}\text{C}^\alpha$ ,  $^{13}\text{C}^\beta$ , and even more so, carbonyl  $^{13}\text{CO}$  of alanine amide all show substantial chemical shift changes upon deprotonation of the  $\alpha$ -aminium group (Brown et al. 1978; Led and Petersen 1979; Quirt et al. 1974; Rabenstein and Sayer 1976a; Surprenant et al. 1980). Thus, when monitored by  $^{13}\text{C}$ -HSQC or  $\text{H}^\alpha(\text{C}^\alpha)\text{CO}$ -type experiments (Kay 1993; Oda et al. 1994), respectively, these nuclei should also serve as reliable reporters for measuring the  $pK_a$  value of the N-terminus of a protein. (Complex heteronuclear NMR experiments are denoted following a loose convention of specifying the measured nuclei, and indicating additional nuclei used for key coupling steps within parentheses). Although not studied herein, upon  $\alpha$ -aminium deprotonation, additional side chain  $^{13}\text{C}$  nuclei in different amino acids are known to show pH-dependent chemical shift changes that vary in sign and magnitude (Quirt et al. 1974; Surprenant et al. 1980). These can also serve as reporter nuclei, as demonstrated by the recent measurement of the  $pK_a$  value of Thr1 in the proteasome core particle, labeled selectively with  $^{13}\text{C}^{\gamma 2}\text{H}_3$ -threonine ( $^{13}\text{C}^{\gamma 2} \Delta\delta \sim -1$  ppm) for methyl-TROSY spectroscopy (Velyvis and Kay 2013).

#### C-terminal carboxylic acid

N-acetyl alanine was used as a model of a C-terminal residue, for which a  $pK_a$  value of 3.55 was measured. The  $^{13}\text{CO}$  of the carboxylic acid functional group shifts downfield by 3.4 ppm upon deprotonation, and thus should be a reliable reporter nucleus for  $pK_a$  measurements via 1D  $^{13}\text{C}$ -NMR or 2D  $\text{H}^\alpha(\text{C}^\alpha)\text{CO}$ -type approaches (Kay 1993; Oda et al. 1994). In addition to significant pH-dependent  $^1\text{H}^\alpha$ ,  $^{13}\text{C}^\alpha$  and  $^{13}\text{C}^\beta$  chemical shift perturbations (Brown

et al. 1978; Led and Petersen 1979; Quirt et al. 1974; Rabenstein and Sayer 1976a; Surprenant et al. 1980), it is also notable that the amide  $^{15}\text{N}$  and  $^1\text{H}^\text{N}$  signals shift downfield by 5.2 ppm and upfield by  $-0.41$  ppm, respectively, when the carboxyl ionizes (Bundi and Wüthrich 1979b). Indeed, the  $^{15}\text{N}$ -HSQC spectrum of a protein often has a sharp, downfield-shifted  $^{15}\text{N}$  signal arising from the amide of its flexible, charged C-terminal residue. Thus,  $^{15}\text{N}$ -HSQC spectra can also be used for  $pK_a$  measurements of a protein's C-terminus, particularly since amide HX will be slow under the acidic conditions likely associated with such a pH titration. This approach was used to determine the  $pK_a \sim 2.7$  for the C-terminal Trp185 of *Bacillus circulans* xylanase (Joshi et al. 1997).

#### Aspartic and glutamic acid

The carboxylic acid functional groups of Asp and Glu in the blocked tripeptides have  $pK_a$  values of 3.86 and 4.34, respectively. With downfield chemical shift changes of 3.2 and 4.1 ppm, respectively, upon deprotonation, the side chain carboxyl  $^{13}\text{C}$  nuclei are most frequently used as reporter nuclei for pH titrations monitored via 1D  $^{13}\text{C}$ -NMR or 2D  $\text{H}_2^{\beta/\gamma}(\text{C}^{\beta/\gamma})\text{CO}^{\gamma/\delta}$  spectra (McIntosh et al. 1996, 2011; Yamazaki et al. 1993, 1994). However, the adjacent aliphatic  $^{13}\text{C}^\beta$  of Asp (3 ppm) and  $^{13}\text{C}^\gamma$  of Glu (3.5 ppm), as well as their directly bonded protons, show comparable chemical shift changes and can also be used for  $pK_a$  measurements (London et al. 1978; Pujato et al. 2006; Quirt et al. 1974; Rabenstein and Sayer 1976a; Richarz and Wüthrich 1978; Yamazaki et al. 1994). This could be accomplished using 2D or 3D versions of the  $\text{H}_2^{\beta/\gamma}\text{C}^{\beta/\gamma}\text{CO}^{\gamma/\delta}$  experiment (Yamazaki et al. 1994). Alternatively, 2D  $^{13}\text{C}$ -HSQC spectra could be used to observe the  $^{13}\text{C}^{\beta/\gamma}\text{H}_2$  signals. However this latter approach would likely require some form of selective  $^{13}\text{C}$ -Asp or -Glu labeling to avoid spectral overlap from a multitude of additional signals expected with a uniformly labeled protein. Given that both the carboxyl and adjacent aliphatic  $^{13}\text{C}$  nuclei show substantial pH-dependent chemical shift changes, "protonless"  $^{13}\text{C}$ -detected  $\text{C}^{\beta/\gamma}\text{CO}^{\gamma/\delta}$  correlation spectra also provide an effective route for measuring Asp and Glu  $pK_a$  values (Castaneda et al. 2009). Although the most sensitive approaches for NMR data acquisition generally rely on  $^1\text{H}$ -detection, cryogenic probes open the door for the improved observation of such  $^{13}\text{C}$  nuclei (Felli and Brutscher 2009).

Signals from the rapidly exchanging oxygen-bonded  $\text{H}^{\delta 2}$  of Asp or  $\text{H}^{\delta 2}$  of Glu (or the C-terminal  $\alpha$ -carboxylic acid  $\text{H}''$  proton) are very rarely seen in the NMR spectra of proteins. Furthermore, with the exception of  $^2\text{J}_{\text{COH}} \sim 7$  Hz and  $^4\text{J}_{\text{HCCOH}} \sim 1$  Hz measured for acetic acid in liquid Freon at 110 K (Tolstoy et al. 2004), no useful scalar couplings have been reported for these acidic

**Table 2** Useful deuterium isotope shifts for characterizing ionizable functional groups

Amino acid	Exchangeable site <sup>a</sup>	Isotope shift (ppm) <sup>a</sup>
Asp/Glu	$\underline{^{13}\text{C}^{\gamma/\delta}\text{O}_2\text{D}} / \underline{^{13}\text{C}^{\gamma/\delta}\text{O}_2\text{H}}$	0.23 <sup>b</sup>
	$\underline{^{13}\text{C}^{\gamma/\delta}\text{O}_2^-} / \underline{^{13}\text{C}^{\gamma/\delta}\text{O}_2^-}$	0
His	$\underline{^{15}\text{N}^{\delta 1/\epsilon 2}\text{D}^+} / \underline{^{15}\text{N}^{\delta 1/\epsilon 2}\text{H}^+}$	0.95 <sup>c,d</sup>
Cys	$\underline{^{13}\text{C}^{\beta}\text{S}^{\gamma}\text{D}} / \underline{^{13}\text{C}^{\beta}\text{S}^{\gamma}\text{H}}$	0.12 <sup>e</sup>
	$\underline{^{13}\text{C}^{\beta}\text{S}^{\gamma-}} / \underline{^{13}\text{C}^{\beta}\text{S}^{\gamma-}}$	0
Tyr	$\underline{^{13}\text{C}^{\zeta}\text{O}^{\eta}\text{D}} / \underline{^{13}\text{C}^{\zeta}\text{O}^{\eta}\text{H}}$	0.13 <sup>f</sup>
	$\underline{^{13}\text{C}^{\zeta}\text{O}^{\eta-}} / \underline{^{13}\text{C}^{\zeta}\text{O}^{\eta-}}$	0
Lys	$\underline{^{15}\text{N}^{\zeta}\text{D}_3^+} / \underline{^{15}\text{N}^{\zeta}\text{H}_3^+}$	1.05 <sup>g,i</sup>
	$\underline{^{15}\text{N}^{\zeta}\text{D}_2} / \underline{^{15}\text{N}^{\zeta}\text{H}_2}$	~1.9 <sup>h,i</sup>
Arg	$\underline{^{15}\text{N}^{\epsilon}\text{D}^+} / \underline{^{15}\text{N}^{\epsilon}\text{H}^+}$	1.0 <sup>d,j</sup>
	$\underline{^{15}\text{N}^{\epsilon}\text{D}_x} / \underline{^{15}\text{N}^{\epsilon}\text{H}_x}$	1.8 <sup>d,j</sup>
	$\underline{^{15}\text{N}^{\eta}\text{D}_2^+} / \underline{^{15}\text{N}^{\eta}\text{H}_2^+}$	1.4 <sup>d,j,k</sup>
	$\underline{^{15}\text{N}^{\eta}\text{D}_y} / \underline{^{15}\text{N}^{\eta}\text{H}_y}$	1.7 <sup>d,j</sup>
	$\underline{^{13}\text{C}^{\zeta}\text{N}^{\epsilon/\eta}\text{D}_5^+} / \underline{^{13}\text{C}^{\zeta}\text{N}^{\epsilon/\eta}\text{H}_5^+}$	0.19 <sup>j</sup>
	$\underline{^{13}\text{C}^{\zeta}\text{N}^{\epsilon/\eta}\text{D}_4} / \underline{^{13}\text{C}^{\zeta}\text{N}^{\epsilon/\eta}\text{H}_4}$	0.08 <sup>j</sup>

<sup>a</sup> Detected nucleus underlined and shift changes are upon transfer from D<sub>2</sub>O to H<sub>2</sub>O. Paired rows correspond to the acid (upper) and conjugate base (lower) forms

<sup>b</sup> From (Ladner et al. 1975; Led and Petersen 1979; Wang et al. 1996). A similar value is expected for the C-terminal carboxylic acid

<sup>c</sup> Average value measured herein at pH/pH\* ~ 3.6 for the imidazolium nitrogens in the blocked histidine tripeptide. Not determined for the neutral side chain due to tautomer averaging

<sup>d</sup> Values due to one-bond and possible three-bond contributions

<sup>e</sup> From (Takeda et al. 2010). The <sup>13</sup>C also experiences three-bond isotope shift upon exchange of the amide D<sup>N</sup> to H<sup>N</sup>

<sup>f</sup> From (Takeda et al. 2009)

<sup>g</sup> Measured herein at pH/pH\* ~ 4, and in agreement with (Tomlinson et al. 2009; Ullah et al. 2011)

<sup>h</sup> Estimated from Δδ of -8.3 and ~ -7.5 ppm upon <sup>15</sup>N<sup>ζ</sup> deprotonation in D<sub>2</sub>O (herein) and H<sub>2</sub>O (Andre et al. 2007), respectively, combined with the total 1.05 ppm deuterium isotope shift for the protonated ζ-aminium of the blocked lysine tripeptide

<sup>i</sup> Isotope shifts of 1.07 ppm for the α-aminium (pH 7 versus pH\* 5.8) and 1.86 ppm for the neutral α-amine (pH 15.25 versus pH\* 15.1) were measured with <sup>13</sup>C/<sup>15</sup>N<sub>4</sub>-L-arginine

<sup>j</sup> Values measured for the side chain of <sup>13</sup>C/<sup>15</sup>N<sub>4</sub>-L-arginine in its guanidinium (pH 7 versus pH\* 5.8) and guanidine (pH 15.25 versus pH\* 15.1) forms. The latter are tautomer averaged and the degree of site-specific protonation (x ≤ 1, y ≤ 2) is undefined

<sup>k</sup> A value of 1.2 ppm was reported by (London et al. 1977)

protons in a polypeptide or protein. Thus, the very limited number of carboxylic acid protons identified to date, which have chemical shifts in the range of ~10 to 22 ppm, appear to have been assigned via homonuclear correlations (e.g., for samples in aprotic solvents (Volpon et al. 2007)) or via perturbations resulting from mutations or ligand

binding (Frey 2001; Hanoian et al. 2010; Langkilde et al. 2008; Saito and Ishikita 2012). However, most of these carboxylic acid-associated protons are also involved in short strong or low barrier hydrogen bonds, for which the predominant role of the Asp/Glu as a proton donor or acceptor is difficult to define.

Although the acidic proton of an Asp, Glu, or C-terminus may be exchanging too rapidly to be detected directly, the observation of a two-bond isotope shift of ~0.23 ppm for the carboxyl carbon (<sup>13</sup>CO<sub>2</sub>H vs. <sup>13</sup>CO<sub>2</sub>D; Table 2) upon transfer from D<sub>2</sub>O to H<sub>2</sub>O provides very good evidence that the functional group is predominantly neutral under the experimental conditions (Ladner et al. 1975; Led and Petersen 1979; Wang et al. 1996). In contrast, the unambiguous lack of an isotope shift indicates that the group is deprotonated (although the α-carboxylate of the C-terminal residue could exhibit a three-bond isotope shift of ~0.03 ppm upon protonation of its deuterated amide (Ladner et al. 1975). Such deuterium isotope shifts are particularly useful when other reporter nuclei do not show a titration, making it unclear if the carboxylic acid has a pK<sub>a</sub> less than the lowest or greater than the highest pH tested (Joshi et al. 1997). Under conditions when the carboxylic acid is neutral (pH ≪ pK<sub>a</sub>), intermediate deuterium isotope shifts might result from strong hydrogen bonding (Dziembowska and Rozwadowski 2001; Guo et al. 2012; Hansen 2007; Joshi et al. 2000).

It is also noteworthy that the <sup>1</sup>J<sub>CC</sub> ~ 50 Hz to the side chain carboxyl of Asp/Glu and to the C-terminal carboxyl decrease by ~3 to 4 and ~6 Hz, respectively, upon deprotonation (London et al. 1978). This offers another possible route for pK<sub>a</sub> measurements and ionization state determination.

## Histidine

Histidine is undoubtedly the most studied ionizable amino acid by NMR spectroscopists for many reasons. These include its frequent roles in ligand binding and enzymatic catalysis, its ionization typically occurring over a physiological pH range (blocked tripeptide pK<sub>a</sub> 6.45), and its wealth of reporter nuclei. Early studies of histidines in proteins often focused on the aromatic carbon-bonded <sup>1</sup>H<sup>δ2</sup> and <sup>1</sup>H<sup>ε1</sup>, which shift upfield by ~ -0.3 and -0.9 ppm, respectively, upon deprotonation (Markley 1975). However, essentially all of the <sup>15</sup>N and <sup>13</sup>C nuclei in this amino acid show substantial pH-dependent chemical shift and J-coupling changes. In particular, the ring <sup>15</sup>N<sup>δ1</sup> and <sup>15</sup>N<sup>ε2</sup> have dramatically different chemical shifts whether protonated or deprotonated (or post-translationally modified, including phosphorylation (Rajagopal et al. 1994; van Dijk et al. 1990)), thus providing very strong evidence for the ionization state of a histidine side chain (Blomberg et al.

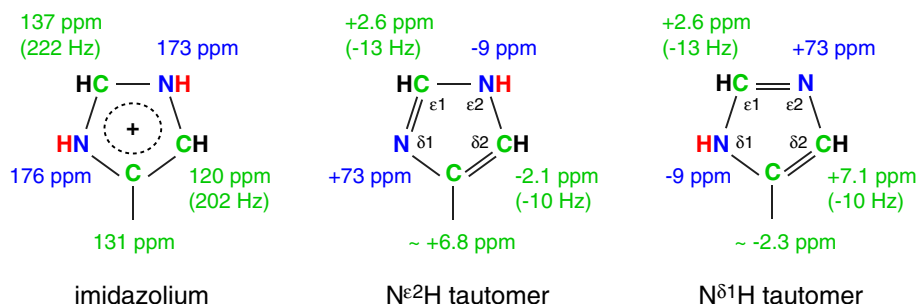


**Fig. 2** Determining the charge and tautomeric state of a histidine. (left) Chemical shifts and  $^1\text{J}_{\text{CH}}$  couplings of the ring  $^{13}\text{C}$  (green) and  $^{15}\text{N}$  (blue) nuclei in the protonated side chain (protons, red and black). Also shown are the chemical shift and J-coupling changes upon deprotonation to the N $\epsilon^2$ H (middle) or N $\delta^1$ H (right) neutral tautomer. The data are from Table 1 or averaged for model compounds reported in the following references for  $^{15}\text{N}$  shifts (Bachovchin 1986; Bachovchin and Roberts 1978; Blomberg et al. 1977; Munowitz

et al. 1982; Pelton et al. 1993; Roberts et al. 1982; Witanowski et al. 1972),  $^{13}\text{C}$  shifts (Goux and Allerhand 1979; Quirt et al. 1974; Reynolds et al. 1973; Reynolds and Tzeng 1977), and  $^1\text{J}_{\text{CH}}$  (Bachovchin et al. 1981; Day et al. 2003; Hansen and Kay 2014; Hunkapiler et al. 1973; Wasylishen and Tomlinson 1975). The  $^1\text{J}_{\text{CH}}$  coupling for  $^{13}\text{C}^{\epsilon 1}$  has been confirmed to be essentially independent of tautomer form (Hansen and Kay 2014), and a similar behavior for  $^{13}\text{C}^{\delta 2}$  is assumed

1977; Kawano and Kyogoku 1975). Accordingly, a wide variety of 1D  $^1\text{H}$ -,  $^{13}\text{C}$ -, and  $^{15}\text{N}$ -NMR or 2D single- and multiple-bond heteronuclear correlation experiments can be used to measure histidine  $\text{pK}_a$  values (Betz et al. 2004; Löhr et al. 2002, 2005; Ludwiczek et al. 2013; Pelton et al. 1993; Plesniak et al. 1996; Schubert et al. 2007; Spitzner et al. 2001; Sudmeier et al. 1996; Yu and Fesik 1994). Although the labile nitrogen-bonded  $^1\text{H}^{\delta 1}$  and  $^1\text{H}^{\epsilon 2}$  of a random coil histidine exchange rapidly with water, when sufficiently protected from HX within a folded protein, they also yield signals typically downfield of 10 ppm. These rather distinct signals are readily detectable in 1D  $^1\text{H}$ -NMR or 2D  $^{15}\text{N}$ -HSQC spectra (Bachovchin 1985; Connelly and McIntosh 1998; Plesniak et al. 1996; Robillard and Shulman 1972; Schubert et al. 2007; Wu et al. 1984).

The neutral imidazole of histidine exists in a pH-independent equilibrium between two tautomers, with the N $\epsilon^2$ H form favored by  $\sim 4$  to 7-fold over the N $\delta^1$ H form in the free amino acid (Blomberg et al. 1977). However, this equilibrium can be readily perturbed by interactions such as hydrogen bonding, and thus it is often important to determine the tautomeric state of a neutral histidine in given protein. Based on NMR spectroscopic studies of several histidine derivatives (Fig. 2), upon neutralization of the imidazolium ring, the  $^{15}\text{N}$  that retains a proton shifts by  $\sim -9$  ppm, whereas the deprotonated  $^{15}\text{N}$  shifts dramatically by  $\sim 73$  ppm (Bachovchin 1986; Bachovchin and Roberts 1978; Munowitz et al. 1982; Roberts et al. 1982; Witanowski et al. 1972). Therefore, the tautomeric state (or equilibrium distribution of tautomers) of a neutral histidine can be deduced immediately upon assignment of its ring  $^{15}\text{N}$  signals. Although obtainable via  $^1\text{H}/^{13}\text{C}/^{15}\text{N}$  triple resonance experiments (Löhr et al. 2005; Sudmeier et al. 1996), these assignments are most frequently determined

using qualitative patterns of small pH-dependent two- and three-bond  $^1\text{H}$ - $^{15}\text{N}$  scalar couplings detected in long-range  $^{15}\text{N}$ -HSQC or  $^{15}\text{N}$ -HMBC spectra (Blomberg et al. 1977; Pelton et al. 1993). A one-bond deuterium isotope shift of  $\sim 0.95$  ppm on the ring nitrogens (Table 2) could also be used to identify the charge and tautomeric state of a histidine. However, given that  $^{15}\text{N}$  shift alone is so diagnostic of protonation, deuterium isotope shift measurements may be more useful for probing other histidine properties, such as hydrogen bonding and HX kinetics (Chevelkov et al. 2010; Tugarinov 2014). In the case of a detectable nitrogen-bonded proton, the magnitude of  $^1\text{J}_{\text{N}\delta^1\text{H}}$  may also correlate to the neutral N $\delta^1$ H tautomer ( $>97$  Hz) or charged imidazolium form ( $<94$  Hz), whereas  $^1\text{J}_{\text{N}\epsilon^2\text{H}}$  appears to be uniformly  $\sim 99$  Hz regardless of charge (Schubert et al. 2007). However, this correlation is derived from a very limited data set and is unlikely to be a robust criterion for determining the tautomerization state of a histidine due to additional structure-dependent factors that could affect these couplings (Bachovchin 2001).

Histidine ionization and tautomerization can also be determined by measuring the chemical shifts of the ring  $^{13}\text{C}$  nuclei using direct  $^{13}\text{C}$  or indirect  $^1\text{H}$ - $^{13}\text{C}$  heteronuclear correlation approaches (Ludwiczek et al. 2013). These are generally more sensitive than the  $^{15}\text{N}$ -directed experiments discussed above. Again, based on model compounds (Fig. 2), deprotonation of the histidine side chain to its N $\epsilon^2$ H tautomer leads to chemical shift changes of approximately 6.5 to 6.8 ppm for the  $^{13}\text{C}^{\gamma}$  nucleus and  $-2.1$  ppm for the  $^{13}\text{C}^{\delta 2}$ , whereas the opposite changes of  $-2.3$  to  $-2.5$  and 7.1 ppm, respectively, result upon formation of its N $\delta^1$ H tautomer (Goux and Allerhand 1979; Reynolds et al. 1973). Thus, the difference between the chemical shift changes exhibited by these two nuclei with increasing pH provides a robust indication of the resulting tautomeric distribution of a given

histidine. Consistent with these data, it has been noted that a  $^{13}\text{C}^{\delta 2}$  chemical shift  $>122$  ppm is diagnostic of a predominant  $\text{N}^{\delta 1}\text{H}$  tautomer (Sudmeier et al. 2003). Parenthetically, due to its sensitivity to tautomerization,  $^{13}\text{C}^{\delta 2}$  shift is a reliable signature of the zinc coordination mode of a histidine (Barraud et al. 2012). Two- and three-bond  $^1\text{H}$ - $^{13}\text{C}$  scalar couplings (Wasylishen and Tomlinson 1977), as well as one-bond  $^{13}\text{C}$ - $^{15}\text{N}$  couplings (Alej et al. 1980; Blomberg et al. 1977; Shimba et al. 1998; Sudmeier et al. 1996) within the imidazole ring can also be used to distinguish histidine tautomers. In contrast, the chemical shifts of carbon-bonded  $^1\text{H}^{\delta 2}$  and  $^1\text{H}^{\epsilon 1}$  alone are not useful reporters of tautomerization (Tanokura 1983). The readily measurable strong  $^1\text{J}_{\text{CH}}$  couplings ( $\sim 200$  Hz) of the ring  $^{13}\text{C}^{\epsilon 1}$  and  $^{13}\text{C}^{\delta 2}$  also decrease by  $\sim 10$  Hz upon deprotonation with little apparent dependence upon tautomeric state (Fig. 2). This provides a complementary route for  $\text{pK}_a$  measurements and ionization state determination (Bachovchin et al. 1981; Day et al. 2003; Hunkapiler et al. 1973; Wasylishen and Tomlinson 1975). Indeed, this coupling has been exploited to measure the  $\text{pK}_a$  values of histidines in sparsely populated unfolded states of proteins (Hansen and Kay 2014). Solid-state NMR methods have also been developed to characterize the charged form and the neutral tautomers of histidine (Li and Hong 2011; Miao et al. 2014).

As a closing point, the values listed in Fig. 1 and Table 1 for the blocked Gly-His-Gly tripeptide are tautomer averaged. Assuming fast exchange between the limiting  $^{15}\text{N}$  and  $^{13}\text{C}$  chemical shift changes of Fig. 2, the neutral histidine in the tripeptide is in equilibrium between major  $\text{N}^{\epsilon 2}\text{H}$  ( $\sim 80\%$ ) and minor  $\text{N}^{\delta 1}\text{H}$  ( $\sim 20\%$ ) forms. Accordingly, the observed macroscopic  $\text{pK}_a$  of 6.45 for deprotonation of either nitrogen is a weighted sum of the microscopic  $\text{pK}_a$  values of 6.55 and 7.15 for forming these two species, respectively (Tanokura 1983).

### Cysteine

The side chain thiol of cysteine in the blocked tripeptide has a  $\text{pK}_a$  value of 8.49. In addition to having highly diagnostic chemical shifts for a disulfide-bridged side chain ( $\sim 41$  ppm) versus a reduced thiol ( $\sim 28$  ppm) (Wishart 2011), the  $^{13}\text{C}^{\beta}$  signal moves downfield by 1.67 ppm upon deprotonation to the thiolate anion. Accordingly, the  $\text{pK}_a$  values of cysteines in several proteins selectively labeled with  $^{13}\text{C}^{\beta}$ -Cys have been measured via  $^{13}\text{C}$ -HSQC approaches (Chivers et al. 1997; Jeng et al. 1995; Mavridou et al. 2007; Mossner et al. 2000; Roos et al. 2013; Wilson et al. 1995). It is notable that the  $^1\text{H}^{\alpha}$ ,  $^{13}\text{C}^{\alpha}$  and amide  $^{15}\text{N}$  show even larger pH-dependent chemical shift changes and thus can also be used as reporter nuclei (Forman-Kay et al. 1992). However, under the alkaline conditions likely associated with cysteine deprotonation, rapid amide HX may well preclude a  $^{15}\text{N}$ -HSQC approach (Lim et al. 2012).

Although the labile sulfur-bonded  $^1\text{H}^{\gamma}$  of cysteine is generally not observable for a random coil polypeptide, it can be detected when protected from rapid HX within the context of a structured protein. Of course, the observation of such a signal provides unambiguous evidence that a cysteine is predominantly in its neutral state. The BioMagResBank (Ulrich et al. 2008) currently lists an average chemical shift of  $2.0 \pm 1.3$  ppm for a small number of thiol  $^1\text{H}^{\gamma}$  signals. However, significant shift deviations are possible depending upon the environment of the proton (Nordstrand et al. 1999). The signals from these slowly-exchanging  $^1\text{H}^{\gamma}$  protons were likely assigned via  $^3\text{J}_{\text{H}\beta\text{H}\gamma}$  scalar (Nordstrand et al. 1999) or interproton NOE interactions (Takeda et al. 2010). Alternatively, by exploiting an expected  $^3\text{J}_{\text{C}\alpha\text{H}\gamma} \sim 3$  to 7 Hz (Hansen 1981), the thiol proton should be detectable and assignable using a long-range  $^{13}\text{C}$ -HSQC experiment as demonstrated for serine/threonine hydroxyl protons (Brockerman et al. 2014). This strategy would likely require selective  $^{13}\text{C}$ -Cys labeling (ideally  $^{13}\text{C}^{\alpha}$  only) because a uniformly enriched protein will yield a myriad of complicated long-range couplings.

The presence of the  $^1\text{H}^{\gamma}$  can be confirmed via a two-bond deuterium isotope shift of  $\sim 0.12$  ppm ( $^{13}\text{C}^{\beta}\text{S}^{\gamma}\text{H}$  vs.  $^{13}\text{C}^{\beta}\text{S}^{\gamma}\text{D}$ ; Table 2) measured via  $^{13}\text{C}$ -NMR in proteins selectively labeled with  $^{13}\text{C}^{\beta}\text{D}_2$ -Cys (Takeda et al. 2010). This isotope shift has also been exploited to quantitate HX rates and protium-deuterium fractionation factors for the thiol moiety (Takeda et al. 2010).

### Tyrosine

Within the context of a blocked tripeptide, tyrosine has a  $\text{pK}_a$  value of 9.76. Thus, this residue is neutral in most proteins under physiological conditions. Upon ionization of the phenolic oxygen, the ring  $^{13}\text{C}^{\gamma}$  and  $^{13}\text{C}^{\zeta}$  shift substantially by  $-6.7$  and  $10.4$  ppm, respectively (Norton and Bradbury 1974; Richarz and Wüthrich 1978). In contrast to the smaller changes exhibited by the other ring  $^{13}\text{C}$  and  $^1\text{H}$  nuclei, these ionization-dependent shift changes are larger than those typically accompanying protein folding or ligand binding (Baturin et al. 2011). Therefore, the  $^{13}\text{C}^{\gamma}$  and  $^{13}\text{C}^{\zeta}$  both serve as very reliable reporter nuclei for  $\text{pK}_a$  measurements. However, neither is directly protonated, thus requiring lower sensitivity approaches such as 2D  $\text{H}^{\epsilon}(\text{C}^{\epsilon})\text{C}^{\zeta}$  or  $\text{H}_2^{\beta}(\text{C}^{\beta})\text{C}^{\gamma}$  correlation spectroscopy (Baturin et al. 2011; Oktaviani et al. 2012; Prompers et al. 1998; Yamazaki et al. 1993).

As with other oxygen-bonded protons, the labile  $^1\text{H}^{\eta}$  of tyrosine is usually observable only when protected from rapid HX, such as via hydrogen bonding within a folded protein (Liepinsh and Otting 1996; Liepinsh et al. 1992). Although the BioMagResBank (Ulrich et al. 2008) lists an average chemical shift of  $9.3 \pm 1.3$  ppm for a small

number of assigned  $^1\text{H}^\eta$  signals, a substantially larger range is possible depending on the structural environment of the tyrosine (Baturin et al. 2011; Werner et al. 1997). In addition to homonuclear NOE approaches, one unambiguous method to assign these signals relies on a weak dihedral angle-dependent  $^3J_{\text{C}^\epsilon\text{H}^\eta}$  coupling of  $\sim 4$  to 8 Hz (Borisov et al. 1998; Bystrov 1976; Hansen 1981) that is detectable in long range  $^{13}\text{C}$ -HSQC spectra (Baturin et al. 2011; Werner et al. 1997). The observation of the  $^1\text{H}^\eta$  either directly or indirectly via a two-bond deuterium isotope shift of  $\sim 0.13$  ppm ( $^{13}\text{C}^\epsilon\text{O}^\eta\text{H}$  vs.  $^{13}\text{C}^\epsilon\text{O}^\eta\text{D}$ ; Table 2) (Takeda et al. 2009) also provides clear evidence that a tyrosine is neutral. Once detected, NOE and J-coupling measurements can be used to obtain distance and dihedral angle restraints, respectively, to define the structural features of tyrosine  $^1\text{H}^\eta$  protons in proteins. Complementary HX studies can be carried out to help characterize their dynamic properties (Baturin et al. 2011; Liepinsh et al. 1992; Takeda et al. 2009).

## Lysine

Lysine in the blocked tripeptide has a  $\text{pK}_a$  value of 10.34. Hence, unless in a highly unusual environment, lysine  $\text{N}^\zeta$ -amino groups in proteins are most likely positively-charged under neutral pH conditions (Daopin et al. 1991; Isom et al. 2011). Similar to an N-terminal amine, the lysine side chain  $^{15}\text{N}^\zeta$  shifts by  $\sim -7.5$  ppm upon deprotonation (Andre et al. 2007), thus allowing reliable  $\text{pK}_a$  measurements by 1D  $^{15}\text{N}$ -NMR (Zhu et al. 1995) or 2D  $\text{H}_2(\text{C}^\epsilon)\text{N}^\zeta$  approaches (Andre et al. 2007; Tomlinson et al. 2009; Yamazaki et al. 1993). In contrast to changes of  $-0.4$  and  $-0.24$  ppm for the non-labile  $^1\text{H}^\epsilon$  and  $^1\text{H}^\delta$ , respectively, and a change of only 1 ppm for the nitrogen-bonded  $^{13}\text{C}^\epsilon$ , the “once removed”  $^{13}\text{C}^\delta$  shifts substantially by 5 ppm upon lysine neutralization (Batchelor et al. 1975; Keim et al. 1974; Kesvatera et al. 1996; Richarz and Wüthrich 1978; Surprenant et al. 1980). Thus, as exemplified by studies of the lyase domain of DNA Pol  $\beta$  (Gao et al. 2006), the  $^{13}\text{C}^\delta$  aliphatic carbon can be used as a very reliable reporter nucleus for  $\text{pK}_a$  measurements via sensitive 2D  $^{13}\text{C}$ -HSQC experiments. However, selective labeling with  $^{13}\text{C}$ -lysine (ideally  $^{13}\text{C}^\delta$  only) is likely required to avoid spectral overlap with other side chain signals, as would arise with a uniformly  $^{13}\text{C}$ -enriched protein.

The labile amino protons of lysines (or the N-terminal amine) can also be observed directly, particularly when protected from rapid HX due to their environment within a folded protein and/or under conditions of low temperature, pH, and general acid/base concentration (Esadze et al. 2014; Iwahara et al. 2007; Liepinsh and Otting 1996; Liepinsh et al. 1992; Poon et al. 2006; Zandarashvili et al.

2013). Strikingly, a chemical shift of 0.8 ppm has been reported for the nitrogen-bonded  $^1\text{H}^\zeta$  of a neutral buried lysine in a staphylococcal nuclease mutant (Takayama et al. 2008a). This stands in contrast to a shift of  $\sim 7.5$  ppm typically found for the protons in the charged  $\zeta$ -aminium group. Thus, if detectable, the  $^1\text{H}^\zeta$  chemical shift of a lysine side chain will be highly diagnostic of its charge state. Alternatively, the  $^{15}\text{N}$  nuclei in  $^{-15}\text{NH}_3^+$  versus  $^{-15}\text{NH}_2$  groups show distinctly different multiplet patterns due to  $^1J_{\text{NH}}$  couplings of  $\sim 74$  Hz (quartet) and  $\sim 64$  Hz (triplet), respectively (Poon et al. 2006; Takayama et al. 2008a, b; Tomlinson et al. 2009). This provides unambiguous evidence for the protonation of a lysine residue. The detection of the lysine  $^{-15}\text{NH}_3^+$  also opens the doors to dynamic studies of this side chain in proteins and protein complexes (Anderson et al. 2013; Esadze et al. 2011; Zandarashvili et al. 2011, 2013).

The lysine  $^{15}\text{N}^\zeta$  aminium group has a combined one-bond deuterium isotope shift of  $3 \times 0.35 = 1.05$  ppm ( $^{15}\text{NH}_3^+$  vs.  $^{15}\text{ND}_3^+$ ; Table 2) (Tomlinson et al. 2009). In contrast, a value of  $\sim 2 \times 0.95 = 1.9$  ppm can be estimated for the combined isotope shift of  $^{-15}\text{NH}_2$  versus  $^{-15}\text{ND}_2$  in the neutral amine (Table 2). Similar results were found for the  $\alpha$ -amine of  $^{13}\text{C}/^{15}\text{N}$ -arginine (Table 2). Therefore the deuterium isotope shifts, which reflect electronic structure and bonding (Hansen 2000), are substantially different for the cationic and neutral states of the lysine  $^{15}\text{N}^\zeta$  nucleus and the N-terminal amine. This parallels data reported for the ammonium ion versus ammonia (Wasylishen and Friedrich 1987). Smaller pH-dependent changes in the multiple-bond deuterium isotope shifts on the side chain  $^{13}\text{C}$  nuclei of lysine have also been measured (Led and Petersen 1979). However, it may be difficult to use deuterium isotope shifts as a criterion for characterizing the charge of a lysine or N-terminus because they also vary with hydrogen bonding and counterions (Hansen and Lycka 1989; Tomlinson et al. 2009; Ullah et al. 2011). This stands in contrast to the simple presence or absence of a deuterium isotope shift for the carboxyl, thiol, and hydroxyl groups in their neutral versus anionic states, respectively.

## Arginine

The  $\text{pK}_a$  value of the arginine side chain has recently been measured as 13.9 (in preparation). This is considerably higher than the commonly cited values of  $\sim 12$  to 12.5 (Creighton 2010), and thus arginines are invariably positively-charged in proteins under physiological conditions. To the best of our knowledge, an arginine in a measurably populated neutral state has never been unambiguously observed within the context of a protein or protein complex, and hence a corresponding  $\text{pK}_a$  value has never been

determined (Baillargeon et al. 1980; Grissom et al. 1987; Harms et al. 2011; Xiao and Braiman 2005). Nevertheless, such studies are very interesting to pursue, particularly for proteins in which the guanidinium moiety becomes post-translationally modified (Smith and Denu 2009) or is potentially involved in a proton transfer cascade (Hutson et al. 2000; McMahon et al. 2004; Petkova et al. 1999; Xiao et al. 2004), or for enzymes that appear to use this side chain as a general acid/base catalyst (Schlippe and Hedstrom 2005). As with all  $pK_a$  measurements, control experiments would be absolutely necessary to ensure that the protein remains in its native state and not hydrolyzed or otherwise chemically modified over the entire pH titration range studied (which, for most systems, seems unlikely given the extreme alkaline conditions required for arginine deprotonation).

Arginine side chains have been characterized extensively with NMR spectroscopy, although almost always in the cationic state (Blomberg et al. 1976; Blomberg and Rüterjans 1983; Kanamori et al. 1978; Kanamori and Roberts 1983; Keim et al. 1974; Legerton et al. 1981; London et al. 1977; Oldfield et al. 1975a, b; Pregosin et al. 1971; Richards and Thomas 1974; Richarz and Wüthrich 1978; Surprenant et al. 1980; Yavari and Roberts 1978). To enable this characterization, many pulse sequences have been developed to detect and assign the  $^1\text{H}$ ,  $^{13}\text{C}$ , and  $^{15}\text{N}$  signals of the guanidinium moiety (Andre et al. 2007; Iwahara and Clore 2006; Pellecchia et al. 1997; Rao et al. 1996; Vis et al. 1994; Wittekind et al. 1993; Yamazaki et al. 1993, 1995). In particular, due to strong  $^1\text{J}_{\text{N}^\epsilon\text{H}}$  and  $^1\text{J}_{\text{N}^\eta\text{H}}$  couplings of  $\sim 93$  Hz, the nitrogen-bonded protons of arginines are often readily observable in  $^{15}\text{N}$ -HSQC spectra recorded under conditions to minimize HX. However, unless restrained by interactions such as hydrogen bonding, rotation about the  $\text{N}^\epsilon\text{-C}^\zeta$  and  $\text{C}^\zeta\text{-N}^\eta$  partial double bonds generally leads to broad, degenerate signals from the two  $^{15}\text{N}^\eta$  and four  $^1\text{H}^\eta$  nuclei (Henry and Sykes 1995; Kanamori and Roberts 1983). Note that, due to this conjugated bonding, the guanidinium group is planar (Raczynska et al. 2003).

We initially attempted to measure the  $pK_a$  value and pH-dependent chemical shift changes of the guanidinium moiety in a blocked tripeptide. However, due to hydrolysis at high pH, reliable data could only be obtained for the side chain  $^{13}\text{C}^\zeta$  and  $^1\text{H}^\delta$  nuclei (Supplemental Table S1). Therefore, we used a sample of  $^{13}\text{C}_6/^{15}\text{N}_4$ -arginine to obtain the desired results, which after correction for shift perturbations due to the titration of the  $\alpha$ -amine (Supplemental Table S2), agreed well with those for the tripeptide. As summarized in Fig. 1 and Table 1, the  $^{13}\text{C}^\zeta$ ,  $^{15}\text{N}^\epsilon$ , and  $^{15}\text{N}^\eta$  all show substantial chemical shift changes upon deprotonation, and thus serve as potential reporter nuclei for arginine  $pK_a$  measurements. The titration  $\Delta\delta$  values

measured herein for these nuclei are consistent with, but generally larger in magnitude, than those published previously (Baillargeon et al. 1980; Kanamori et al. 1978; Kanamori and Roberts 1983; London et al. 1977; Suzuki et al. 1974; Xiao and Braiman 2005). This is most likely due to difficulties in extrapolation to high pH plateau chemical shifts. Alternatively, since arginine can dimerize (Kubickova et al. 2011; Vondrasek et al. 2009), this might reflect differences in experimental conditions. However, similar shift changes were determined with 10 and 100 mM samples. Under highly alkaline conditions, the guanidinium protons will undergo rapid HX, and thus these reporter nuclei would have to be observed by directly via  $^{15}\text{N}$ - or  $^{13}\text{C}$ -NMR or indirectly via scalar correlations with the non-exchangeable side chain protons. Observing the  $^{15}\text{N}^\eta$  nuclei would be most challenging due to their terminal positions and potentially broad signals resulting from rotation about the  $\text{N}^\epsilon\text{-C}^\zeta$  bond or from tautomerization (Kanamori and Roberts 1983). This is unfortunate as the  $^{15}\text{N}^\eta$  nuclei, with dramatically different chemical shifts of  $\sim 71$  and  $93$  ppm in charged versus neutral arginine, should best serve as reporters of its ionization state. However, any arginine with an unusually low  $pK_a$  value will likely be in a very unusual environment, which may also lead to strongly perturbed chemical shifts. Indeed, the chemical shift differences between the charged and neutral arginine side chain nitrogens are substantially smaller in nonpolar solvents than in water (Xiao and Braiman 2005).

It is also worth noting that the neutral side chain guanidine moiety is non-planar and can exist in five possible tautomeric forms, each lacking one of the five different nitrogen-bonded protons (Raczynska et al. 2003). Experimental (Kanamori and Roberts 1983) and theoretical calculations (Norberg et al. 2005) suggest that these tautomers, which can interconvert rapidly via bond rotations or proton transfer, are roughly iso-energetic and exist in an equilibrium distribution with  $\sim 1/3$  deprotonated at  $\text{N}^\epsilon$ . This is also supported by the observation that the  $^{15}\text{N}^\epsilon$  and two  $^{15}\text{N}^\eta$  nuclei still have similar chemical shifts in the deprotonated state of  $^{13}\text{C}_6/^{15}\text{N}_4$ -arginine (with the  $^{15}\text{N}^\eta$  being degenerate). Significantly different shifts would be expected for non-interconverting  $\text{sp}^2$  ( $\text{C}=\text{N}$  bonded) and  $\text{sp}^3$  ( $\text{C}-\text{N}$  bonded) hybridized nitrogens (Witanowski et al. 1976).

To test this prediction, we also measured deuterium isotope shifts for the  $^{15}\text{N}^\epsilon$  and  $^{15}\text{N}^\eta$  nuclei. Based on comparative titrations of  $^{13}\text{C}_6/^{15}\text{N}_4$ -arginine in  $\text{H}_2\text{O}$  and  $\text{D}_2\text{O}$ , at low (high) pH, deuterium isotope shifts of 1.0 ppm (1.8 ppm) were measured for the  $^{15}\text{N}^\epsilon$  and 1.4 ppm (1.7 ppm) were measured for the  $^{15}\text{N}^\eta$  (Table 2). Thus, as seen with the amino group, deuterium isotope shifts are generally larger for the neutral guanidine than the charged guanidinium species despite the reduced number of

hydrogens. However, these measurements are complicated by possible incomplete (and differing levels of) deprotonation under extremely high pH conditions, particularly since pH meter readings and the  $pK_a$  value of arginine likely differ in  $H_2O$  versus  $D_2O$  solutions (Krezel and Bal 2004). In addition, multiple three-bond isotope shifts could add to the one-bond shifts. Although many such caveats exist, these measurements do indicate that the  $N^{\epsilon}$  and  $N^{\eta}$  nuclei all remain at least partially protonated in the neutral tautomers of free arginine. Of course, if indeed present in a folded protein, the relative populations of these tautomers could change in response to structure-dependent intermolecular interactions, such as hydrogen bonding. Conversely, without better characterization, deuterium isotope shift measurements are not likely useful for determining the charge and tautomeric form of an arginine side chain, even if restrained within a protein.

### Phosphoamino acids

For completeness, we have also included the pH-dependent chemical shift changes of phosphoserine (second  $pK_a$  5.96), phosphothreonine ( $pK_a$  6.30) and phosphotyrosine ( $pK_a$  5.96) in Fig. 1. These data were measured by Bienkiewicz and Lumb for these commonly phosphorylated amino acids (X) in the context of the blocked pentapeptide, acetyl-Gly-Gly-X-Gly-Gly-amide at 25 °C (Bienkiewicz and Lumb 1999). Similar results were reported earlier for unblocked Gly-Gly-X-Ala peptides containing these three phosphoamino acids (Hoffmann et al. 1994). Data have also been published for phosphohistidine (Kalbitzer and Rosch 1981) and phosphoaspartate (Schlemmer et al. 1988).

Certainly,  $^{31}P$ -NMR monitored pH-titrations of the phosphate moieties provide an obvious route for  $pK_a$  measurements. However, several  $^1H$ ,  $^{13}C$  and  $^{15}N$  nuclei in these amino acids show diagnostic changes upon phosphorylation, as well as upon deprotonation to the dianion. The former can be used to identify modification sites within a protein (Bienkiewicz and Lumb 1999; Hoffmann et al. 1994; Lau et al. 2012; McIntosh et al. 2009; Smet-Nocca et al. 2013), whereas the latter can also be monitored for  $pK_a$  measurements. Akin to phosphorylation, many additional post-translational modifications involve ionizable side chains or introduce ionizable groups into protein. These can also be characterized by NMR spectroscopy, including biologically relevant *in vivo* approaches (Theillet et al. 2012).

### Amides

The main chain amide  $^1H^N$ ,  $^{15}N$  and  $^{13}CO$  nuclei of the blocked tripeptides exhibit chemical shift changes due to

side chain deprotonation. As expected for both through-bond inductive and through-space electric field interactions, the magnitudes of these changes generally increase with decreasing separation to the acid/base functional group. Thus, the intra-residue  $^1H^N$  and  $^{15}N$  of the peptide preceding and the  $^{13}CO$  of the peptide following the ionizable side chain show the largest pH-dependent shift perturbations, whereas the flanking glycines report smaller changes. Nevertheless, the latter nearest-neighbor amide titration shifts can still be substantial, particularly for Asp, His, and Cys (Fig. 1 and Supplemental Table S1). It is also interesting that the intra-residue  $^1H^N$  signal of *N*-acetyl alanine, Asp, His, and Cys shift upfield upon deprotonation, whereas those of Glu, phosphoserine, and phosphothreonine shift downfield. In the case of Glu, the downfield shift has been attributed to a transient intra-residue hydrogen bond between the amide and the  $\delta$ -carboxyl that strengthens when the latter is deprotonated (Bundi and Wüthrich 1979b; Mayer et al. 1979). Similar seven-membered rings could be formed by the two phosphorylated amino acids.

The amide  $^{15}N$ -HSQC spectrum of a protein serves as its “fingerprint” due to the presence of one  $^1H^N$ - $^{15}N$  crosspeak from each non-proline or non-N-terminal residue that does not undergo rapid HX. Robust methods have also been developed to rapidly assign the signals from the mainchain  $^1H$ ,  $^{13}C$  and  $^{15}N$  nuclei of a protein, which in turn are stepping stones to its side chain nuclei (Sattler et al. 1999). Accordingly, it is often simple and convenient to monitor the pH-titration of a protein using  $^{15}N$ -HSQC or HNCOType spectra. Indeed, in numerous cases,  $pK_a$  values of ionizable groups have been extracted from pH-dependent intra-residue and nearest-neighbor amide  $^1H^N$ ,  $^{15}N$  and, to a lesser extent,  $^{13}CO$  shifts in both folded (Anderson et al. 1993; Betz et al. 2004; Forman-Kay et al. 1992; Lindman et al. 2007; Tomlinson et al. 2010) and unfolded proteins (Pujato et al. 2006). However, caution must be exercised in interpreting such data because the amide of an acid/base residue may also report the ionization of other residues in a folded protein. Indeed, amides of non-titrating residues often show pronounced apparent titrations that can arise from many reasons. In addition to pH-dependent structural changes (Kukic et al. 2010; Tomlinson et al. 2010), inter-residue hydrogen bonding between an amide and an ionizable side chain can lead to diagnostic downfield  $^1H^N$  shift changes upon deprotonation (Betz et al. 2004; Clark et al. 2007; Ebina and Wüthrich 1984; Haruyama et al. 1989; Khare et al. 1997; Schaller and Robertson 1995). Furthermore, the chemical shifts of the polarizable peptide are particularly sensitive to their local electric fields (Buckingham 1960), and these fields can change upon the titrations of even relatively distal groups in a protein. This sensitivity has been exploited to probe protein

electrostatics, including extracting dielectric constants (An et al. 2014; Boyd et al. 2003; Hass et al. 2008; Kukic et al. 2013).

### Concluding remarks

In this paper, we report the pH-dependent chemical shifts of essentially all the  $^1\text{H}$ ,  $^{13}\text{C}$ , and  $^{15}\text{N}$  nuclei associated with the acid/base functional groups in a protein. The few missing values correspond to the rapidly exchanging protons of the conjugate base forms of the ionizable residues that could not be detected under alkaline conditions. These data, which are consistent with and extend upon those of numerous pioneering studies, were measured in the context of a blocked tripeptide under a common set of experimental conditions. This unified set of reference chemical shifts should help guide protein  $\text{pK}_a$  studies.

Measuring pH-dependent chemical shifts by NMR spectroscopy is often straightforward for a protein, provided that it is well behaved across the necessary experimental conditions. However, interpreting the resulting titration curves to yield residue-specific  $\text{pK}_a$  values and ionization states can be very difficult (Lindman et al. 2006; McIntosh et al. 2011; Søndergaard et al. 2008; Szakacs et al. 2004; Ullmann 2003; Webb et al. 2011). This difficulty results from the complex nature of electrostatic interactions in proteins, combined with the sensitivity of chemical shifts to many pH-dependent factors and the often unappreciated fact that most titration curves are experimentally underdetermined for model fitting (Shrager et al. 1972). The confidence by which one can assign observed titrations to the ionization of a specific residue in a protein certainly increases if several  $^{13}\text{C}$ ,  $^{15}\text{N}$  or non-exchangeable  $^1\text{H}$  nuclei closely associated with that residue all report coincident pH-dependent chemical shift changes. Importantly, these titration shifts should be comparable in sign and magnitude to those exhibited by reference model compounds. Practically speaking, the number of such reporter nuclei that can be monitored will depend upon the pH-dependent stability of the protein combined with feasibility of the required isotopic labeling strategies and the dispersion, resolution and sensitivity (time requirements) of the corresponding NMR experiments. With this said, there are numerous published cases where even directly bonded nuclei within a given residue track very different titrations. These include amide  $^{15}\text{NH}$  (Tomlinson et al. 2010; Webb et al. 2011), Asp, Glu, and Cys  $^{13}\text{CH}_2$  (Jeng et al. 1995; Oda et al. 1994; Song et al. 2003; Wilson et al. 1995), and even His imidazole  $^{13}\text{CH}$  pairs (Ludwiczek et al. 2013). Based on these and other examples, the  $^{15}\text{N}$  and  $^{13}\text{C}$  nuclei are generally the more reliable reporters of intra-residue ionization, whereas the  $^1\text{H}$  are frequently

sensitive to additional pH-dependent changes in the protein.

Unfortunately, the chemical shifts of most reporter nuclei for the protonated and deprotonated forms of the ionizable functional groups fall within the range of chemical shifts induced upon protein folding or ligand binding. For example, the  $^{13}\text{C}^\beta$  and carboxyl  $^{13}\text{C}^\gamma$  of an aspartic acid change from approximately 38 to 41 and 177 to 180 ppm, respectively, upon deprotonation, whereas structure-dependent shifts of 38–44 and 176–183 ppm are listed for these nuclei in the BioMagResBank (Ulrich et al. 2008). The latter values represent the mean chemical shifts  $\pm 2$  standard deviations for all diamagnetic proteins, regardless of sample conditions. The few exceptions to this point include the histidine  $^{15}\text{N}^{\delta 1}$  and  $^{15}\text{N}^{\epsilon 2}$ , tyrosine  $^{13}\text{C}^\gamma$  and  $^{13}\text{C}^\zeta$ , and arginine  $^{15}\text{N}^n$  reporter nuclei, which exhibit rather large, and hence diagnostic, pH-dependent changes in their resonance frequencies. Accordingly, great caution should be exercised in inferring ionization states from chemical shift (or J-coupling) information alone. Strictly speaking, in the absence of a detectable pH titration, one can only conclude that the  $\text{pK}_a$  value of a residue is either less than the lowest sample pH value examined (and thus deprotonated throughout the titration) or greater than the highest pH value examined (protonated). Fortunately, several NMR approaches can be used to resolve this problem by providing complementary insights into the ionization states of protein. In particular, the direct observation of a slowly exchanging acidic proton via chemical shift or J-coupling measurements is clearest evidence that a functional group is in its conjugate acid form. Alternatively, for groups with well-populated but rapidly exchanging acidic protons, deuterium isotope shift measurements can help define their charged states. Of course, parallel studies with biophysical techniques other than NMR spectroscopy can be highly informative.

The reference data provided herein should also help enable pH-dependent corrections in algorithms used to predict the “random coil” chemical shifts of a polypeptide sequence. These reference shifts are of great importance to NMR spectroscopists for numerous reasons, including determining the secondary/tertiary structure and dynamics of a protein or protein complex from chemical shift information, as well as characterizing transient conformations within otherwise intrinsically disordered regions of these biomolecules (Wishart 2011). Broadly speaking, these algorithms have been developed from the statistical analyses of protein chemical shift databases (De Simone et al. 2009; Tamiola et al. 2010; Wang and Jardetzky 2002) or from studies of various reference polypeptides (Braun et al. 1994; Kjaergaard et al. 2011; Prestegard et al. 2013; Schwarzingler et al. 2001; Thanabal et al. 1994; Wishart et al. 1995). The latter were generally

carried out under acidic conditions, and have been adapted to account for the ionization of Asp, Glu, and His. The current tripeptide data provide corrections for the remaining termini and Cys, Tyr, Lys, and Arg residues, as well as an essentially complete summary of the pH-dependent  $^1\text{H}$ ,  $^{13}\text{C}$ , and  $^{15}\text{N}$  chemical shifts of all the main chain and side chain nuclei of these ionizable amino acids in proteins.

**Acknowledgments** G. P. was supported by the Austrian Science Fund (FWF). This research was funded by a Natural Sciences and Engineering Research Council of Canada (NSERC) Discovery Grant to L.P.M. Instrument support was provided by the Canadian Institutes for Health Research (CIHR), the Canadian Foundation for Innovation (CFI), the British Columbia Knowledge Development Fund (BCKDF), the UBC Blusson Fund, and the Michael Smith Foundation for Health Research (MSFHR).

## References

- Alei M, Morgan LO, Wageman WE, Whaley TW (1980) pH-dependence of  $^{15}\text{N}$  NMR shifts and coupling-constants in aqueous imidazole and 1-methylimidazole—comments on estimation of tautomeric equilibrium-constants for aqueous histidine. *J Am Chem Soc* 102:2881–2887
- Alexov E et al (2011) Progress in the prediction of pKa values in proteins. *Proteins* 79:3260–3275
- An L, Wang Y, Zhang N, Yan S, Bax A, Yai L (2014) Protein apparent dielectric constant and its temperature dependence from remote chemical shift effects. *J Am Chem Soc* 136, 9 Sept 2014 [Epub ahead of print]
- Anderson DE, Lu J, McIntosh LP, Dahlquist FW (1993) The folding, stability and dynamics of T4 lysozyme: a perspective using nuclear magnetic resonance. In: Clore GM, Gronenborn AM (eds) *NMR of Proteins*, MacMillan Press, London, pp 258–304
- Anderson KM, Esadze A, Manoharan M, Bruschiweiler R, Gorenstein DG, Iwahara J (2013) Direct observation of the ion-pair dynamics at a protein-DNA interface by NMR spectroscopy. *J Am Chem Soc* 135:3613–3619
- Andre I, Linse S, Mulder FAA (2007) Residue-specific pKa determination of lysine and arginine side chains by indirect  $^{15}\text{N}$  and  $^{13}\text{C}$  NMR spectroscopy: application to apo calmodulin. *J Am Chem Soc* 129:15805–15813
- Bachovchin WW (1985) Confirmation of the assignment of the low-field proton-resonance of serine proteases by using specifically  $^{15}\text{N}$  labeled enzyme. *Proc Natl Acad Sci USA* 82:7948–7951
- Bachovchin WW (1986)  $^{15}\text{N}$  NMR spectroscopy of hydrogen-bonding interactions in the active-site of serine protease—evidence for a moving histidine mechanism. *Biochemistry* 25:7751–7759
- Bachovchin WW (2001) Contributions of NMR spectroscopy to the study of hydrogen bonds in serine protease active sites. *Magn Reson Chem* 39:S199–S213
- Bachovchin WW, Roberts JD (1978)  $^{15}\text{N}$  nuclear magnetic-resonance spectroscopy—state of histidine in catalytic triad of alpha-lytic protease—implications for charge-relay mechanism of peptide-bond cleavage by serine proteases. *J Am Chem Soc* 100:8041–8047
- Bachovchin WW, Kaiser R, Richards JH, Roberts JD (1981) Catalytic mechanism of serine proteases—re-examination of the pH-dependence of the histidyl  $^1\text{J}_{^{13}\text{C}^{\text{H}}}$  coupling-constant in the catalytic triad of alpha-lytic protease. *Proc Natl Acad Sci* 78:7323–7326
- Baillargeon MW, Laskowski M, Neves DE, Porubcan MA, Santini RE, Markley JL (1980) Soybean trypsin-inhibitor (kunitz) and its complex with trypsin— $^{13}\text{C}$  nuclear magnetic-resonance studies of the reactive site arginine. *Biochemistry* 19:5703–5710
- Barraud P, Scubert M, Allain FHT (2012) A strong  $^{13}\text{C}$  chemical shift signature provides the coordination mode of histidines in zinc-binding proteins. *J Biomol NMR* 53:93–101
- Batchelor JG, Feeney J, Roberts GCK (1975)  $^{13}\text{C}$  NMR protonation shifts of amines, carboxylic-acids and amino acids. *J Magn Reson* 20:19–38
- Baturin SJ, Okon M, McIntosh LP (2011) Structure, dynamics, and ionization equilibria of the tyrosine residues in *Bacillus circulans* xylanase. *J Biomol NMR* 51:379–394
- Betz M, Löhr F, Wienk H, Rüterjans H (2004) Long-range nature of the interactions between titratable groups in *Bacillus agaradhaerens* family 11 xylanase: pH titration of *B-agaradhaerens* xylanase. *Biochemistry* 43:5820–5831
- Bienkiewicz EA, Lumb KJ (1999) Random-coil chemical shifts of phosphorylated amino acids. *J Biomol NMR* 15:203–206
- Blakeley MP, Langan P, Niimura N, Podjarny A (2008) Neutron crystallography: opportunities, challenges, and limitations. *Curr Opin Struct Biol* 18:593–600
- Blomberg F, Rüterjans H (1983) Nitrogen-15 NMR in biological systems. *Biol Magn Reson* 21–73
- Blomberg F, Maurer W, Rüterjans H (1976)  $^{15}\text{N}$  nuclear magnetic resonance investigations on amino-acids. *Proc Natl Acad Sci USA* 73:1409–1413
- Blomberg F, Maurer W, Rüterjans H (1977) Nuclear magnetic resonance investigation of  $^{15}\text{N}$ -labeled histidine in aqueous-solution. *J Am Chem Soc* 99:8149–8159
- Borisov EV, Zhang W, Bolvig S, Hansen PE (1998) nJ(13C, O1H) coupling constants of intramolecularly hydrogen-bonded compounds. *Magn Reson Chem* 36:S104–S110
- Boyd J, Domene C, Redfield C, Ferraro MB, Lazzaretto P (2003) Calculation of dipole-shielding polarizabilities ( $\sigma_{\alpha\beta\gamma}^1$ ): the influence of uniform electric field effects on the shielding of backbone nuclei in proteins. *J Am Chem Soc* 125:9556–9557
- Braun D, Wider G, Wüthrich K (1994) Sequence-corrected  $^{15}\text{N}$  random coil chemical shifts. *J Am Chem Soc* 116:8466–8469
- Brockerman JA, Okon M, McIntosh LP (2014) Detection and characterization of serine and threonine hydroxyl protons in *Bacillus circulans* xylanase by NMR spectroscopy. *J Biomol NMR* 58:17–25
- Brown LR, Demarco A, Richarz R, Wagner G, Wüthrich K (1978) Influence of a single salt bridge on static and dynamic features of globular solution conformation of basic pancreatic trypsin-inhibitor— $^1\text{H}$  and  $^{13}\text{C}$  NMR studies of native and transaminated inhibitor. *Eur J Biochem* 88:87–95
- Buckingham AD (1960) Chemical shifts in the nuclear magnetic resonance spectra of molecules containing polar groups. *Can J Chem* 38:300–307
- Bundi A, Wüthrich K (1979a)  $^1\text{H}$ -NMR parameters of the common amino-acid residues measured in aqueous-solutions of the linear tetrapeptides H-Gly-Gly-X-L-Ala-OH. *Biopolymers* 18:285–297
- Bundi A, Wüthrich K (1979b) Use of amide  $^1\text{H}$ -NMR titration shifts for studies of polypeptide conformation. *Biopolymers* 18:299–311
- Bystrov VF (1976) Spin-spin coupling and the conformational states of peptide systems. *Prog Nuc Mag Reson Spect* 10:41–81
- Castaneda CA, Fitch CA, Majumda A, Khangulov V, Schlessman JL, Garcia-Moreno B (2009) Molecular determinants of the pKa values of Asp and Glu residues in staphylococcal nuclease. *Proteins Struct Funct Design* 15:570–588
- Chevelkov V, Xue Y, Rao DK, Forman-Kay JD, Skrynnikov NR (2010)  $^{15}\text{N}$  H/D-SOLEXSY experiment for accurate measurement of amide solvent exchange rates: application to denatured drkN SH3. *J Biomol NMR* 46:227–244

- Chivers PT, Prehoda KE, Volkman BF, Kim B-M, Markley JL, Raines RT (1997) Microscopic pKa values of *Escherichia thio*redoxin. *Biochemistry* 36:14985–14991
- Clark AT, Smith K, Muhandiram R, Edmondson SP, Shriver JW (2007) Carboxyl pKa values, ion pairs, hydrogen bonding, and the pH-dependence of folding the hyperthermophile proteins Sac7d and Sso7d. *J Mol Biol* 372:992–1008
- Cohen JS, Hughes L, Wooten JB (1983) Observations of amino acid side chains in proteins by NMR methods. In: Cohen JS (ed) *Magnetic resonance in biology*, vol 2. Wiley Interscience, New York, pp 130–147
- Connelly GP, McIntosh LP (1998) Characterization of a buried neutral histidine in *Bacillus circulans* xylanase: internal dynamics and interaction with a bound water molecule. *Biochemistry* 37:1810–1818
- Creighton TE (2010) *The biophysical chemistry of nucleic acids and proteins*. Helvetian Press, Oxford
- Daopin S, Anderson DE, Baase WA, Dahlquist FW, Matthews BW (1991) Structural and thermodynamic consequences of burying a charged residue within the hydrophobic core of T4 lysozyme. *Biochemistry* 30:11521–11529
- Day RM et al (2003) Tautomerism, acid-base equilibria, and H-bonding of the six histidines in subtilisin BPN' by NMR. *Protein Sci* 12:794–810
- De Simone A, Cavalli A, Hsu STD, Vranken W, Vendruscolo M (2009) Accurate random coil chemical shifts from an analysis of loop regions in native states of proteins. *J Am Chem Soc* 131:16332–16333
- Demarco A (1977) pH-dependence of internal references. *J Magn Reson* 26:527–528
- Dziembowska T, Rozwadowski Z (2001) Application of the deuterium isotope effect on NMR chemical shift to study proton transfer equilibrium. *Curr Org Chem* 5:289–313
- Ebina S, Wüthrich K (1984) Amide proton titration shifts in bull seminal inhibitor IIa by two-dimensional correlated <sup>1</sup>H nuclear magnetic-resonance (COSY)—manifestation of conformational equilibria involving carboxylate groups. *J Mol Biol* 179:283–288
- Englander SW, Kallenbach NR (1983) Hydrogen exchange and structural dynamics of proteins and nucleic acids. *Q Rev Biophys* 16:521–655
- Esadze A, Li DW, Wang TZ, Bruschiweiler R, Iwahara J (2011) Dynamics of lysine side-chain amino groups in a protein studied by heteronuclear <sup>1</sup>H-<sup>15</sup>N NMR spectroscopy. *J Am Chem Soc* 133:909–919
- Esadze A, Zandarashvili L, Iwahara J (2014) Effective strategy to assign <sup>1</sup>H-<sup>15</sup>N heteronuclear correlation NMR signals from lysine side-chain NH<sub>3</sub><sup>+</sup> groups of proteins at low temperatures. *J Biomol NMR* 60:23–27
- Felli IC, Brutscher B (2009) Recent advances in solution NMR: fast methods and heteronuclear direct detection. *ChemPhysChem* 10:1356–1368
- Fitch CA, Karp DA, Lee KK, Stites WE, Lattman EE, Garcia-Moreno EB (2002) Experimental pKa values of buried residues: analysis with continuum methods and role of water penetration. *Biophys J* 82:3289–3304
- Forman-Kay JD, Clore GM, Gronenborn AM (1992) Relationship between electrostatics and redox function in human thioredoxin—characterization of pH titration shifts using 2-dimensional homonuclear and heteronuclear NMR. *Biochemistry* 31:3442–3452
- Forsyth WR, Antosiewicz JM, Robertson AD (2002) Empirical relationships between protein structure and carboxyl pKa values in proteins. *Proteins Struct Func Bioinform* 48:388–4034
- Freedman MH, Lyster JR, Chaiken IM, Cohen JS (1973) <sup>13</sup>C nuclear magnetic-resonance studies on selected amino acids, and proteins. *Eur J Biochem* 32:215–226
- Frey PA (2001) Strong hydrogen bonding in molecules and enzymatic complexes. *Magn Reson Chem* 39:S190–S198
- Gao GH, Prasad R, Lodwig SN, Unkefer CJ, Beard WA, Wilson SH, London RE (2006) Determination of lysine pK values using [5-<sup>13</sup>C]lysine: application to the lyase domain of DNA Pol β. *J Am Chem Soc* 128:8104–8105
- Goux WJ, Allerhand A (1979) Studies of chemically modified histidine residues of proteins by <sup>13</sup>C nuclear magnetic resonance spectroscopy. Reaction of hen egg white lysozyme with iodoacetate. *J Biol Chem* 254:2210–2213
- Grimsley GR, Scholtz JM, Pace CN (2009) A summary of the measured pK values of the ionizable groups in folded proteins. *Protein Sci* 18:247–251
- Grissom CB, Chinami MA, Benway DA, Ulrich EL, Markley JL (1987) Staphylococcal nuclease active-site amino-acids—pH-dependence of tyrosine and arginine as determined by NMR and kinetic-studies. *Biochemistry* 28:2116–2124
- Gueron M, Plateau P, Decors M (1991) Solvent signal suppression in NMR. *Prog Nuc Mag Reson Spect* 23:135–209
- Guo J, Tolstoy PM, Koeppel B, Golubev NS, Denisov GS, Smirnov SN, Limbach HH (2012) Hydrogen bond geometries and proton tautomerism of homoconjugated anions of carboxylic acids studied via H/D isotope effects on <sup>13</sup>C NMR chemical shifts. *J Phys Chem A* 116:11180–11188
- Hanoian P, Sigala PA, Herschlag D, Hammes-Schiffer S (2010) Hydrogen bonding in the active site of ketosteroid isomerase: electronic inductive effects and hydrogen bond coupling. *Biochemistry* 49:10339–10348
- Hansen PE (1981) Carbon-hydrogen spin-spin coupling-constants. *Prog Nucl Magn Reson Spect* 14:175–296
- Hansen PE (2000) Isotope effects on chemical shifts of proteins and peptides. *Magn Reson Chem* 38:1–10
- Hansen PE (2007) Isotope effect on chemical shifts in hydrogen-bonded systems. *J Labelled Compd Rad* 50:967–981
- Hansen AL, Kay LE (2014) Measurement of histidine pKa values and tautomer populations in invisible protein states. *Proc Natl Acad Sci U S A* 111:E1705–E1712
- Hansen PE, Lycka A (1989) A reinvestigation of one-bond deuterium-isotope effects on nitrogen and on proton nuclear shielding for the ammonium ion. *Acta Chem Scand* 43:222–232
- Harms MJ, Schlessman JL, Sue GR, Garcia-Moreno B (2011) Arginine residues at internal positions in a protein are always charged. *Proc Natl Acad Sci USA* 108:18954–18959
- Harris TK, Turner GJ (2002) Structural basis of perturbed pKa values of catalytic groups in enzyme active sites. *IUBMB life* 53:85–98
- Haruyama H, Qian YQ, Wüthrich K (1989) Static and transient hydrogen-bonding interactions in recombinant desulfatohirudin studied by <sup>1</sup>H nuclear magnetic resonance measurements of amide proton exchange rates and pH-dependent chemical shifts. *Biochemistry* 28:4312–4317
- Hass MA, Jensen MR, Led JJ (2008) Probing electric fields in proteins in solution by NMR spectroscopy. *Proteins* 72:333–343
- Henry GD, Sykes BD (1990) Hydrogen-exchange kinetics in a membrane-protein determined by <sup>15</sup>N NMR spectroscopy—use of the INEPT experiment to follow individual amides in detergent-solubilized M13 coat protein. *Biochemistry* 29:6303–6313
- Henry GD, Sykes BD (1995) Determination of the rotational-dynamics and pH-dependence of the hydrogen-exchange rates of the arginine guanidino group using NMR spectroscopy. *J Biomol NMR* 6:59–66
- Hoffmann R, Reichert I, Wachs WO, Zeppezauer M, Kalbitzer HR (1994) <sup>1</sup>H and <sup>31</sup>P NMR spectroscopy of phosphorylated model peptides. *Int J Pept Protein Res* 44:193–198
- Howarth OW, Lilley DMJ (1978) Carbon-13 NMR of peptides and proteins. *Prog Nuc Magn Reson Spect* 12:1–40

- Hunkapiler MW, Smallcombe SH, Whitaker DR, Richards JH (1973) Carbon nuclear magnetic-resonance studies of histidine residue in alpha-lytic protease—implications for catalytic mechanism of serine proteases. *Biochemistry* 12:4732–4743
- Hutson MS, Alexiev U, Shilov SV, Wise KJ, Braiman MS (2000) Evidence for a perturbation of arginine-82 in the bacteriorhodopsin photocycle from time-resolved infrared spectra. *Biochemistry* 39:13189–13200
- Isom DG, Castaneda CA, Cannon BR, Garcia-Moreno BE (2011) Large shifts in pKa values of lysine residues buried inside a protein. *Proc Natl Acad Sci USA* 108:5260–5265
- Iwahara J, Clore GM (2006) Sensitivity improvement for correlations involving arginine side-chain  $N^{\epsilon}/H^{\epsilon}$  resonances in multi-dimensional NMR experiments using broadband  $^{15}\text{N}$   $180^{\circ}$  pulses. *J Biomol NMR* 36:251–257
- Iwahara J, Jung YS, Clore GM (2007) Heteronuclear NMR spectroscopy for lysine  $\text{NH}_3$  groups in proteins: unique effect of water exchange on  $^{15}\text{N}$  transverse relaxation. *J Am Chem Soc* 129:2971–2980
- Jeng MF, Holmgren A, Dyson HJ (1995) Proton sharing between cysteine thiols in *Escherichia coli* thioredoxin—implications for the mechanism of protein disulfide reduction. *Biochemistry* 34:10101–10105
- Joshi MD, Hedberg A, McIntosh LP (1997) Complete measurement of the pKa values of the carboxyl and imidazole groups in *Bacillus circulans* xylanase. *Protein Sci* 6:2667–2670
- Joshi MD, Sidhu G, Pot I, Brayer GD, Withers SG, McIntosh LP (2000) Hydrogen bonding and catalysis: a novel explanation for how a single amino acid substitution can change the pH optimum of a glycosidase. *J Mol Biol* 299:255–279
- Kalbitzer HR, Rosch P (1981) The effect of phosphorylation of the histidyl residue in the tetrapeptide Gly-Gly-His-Ala—changes of chemical shift and pK values in  $^1\text{H}$ -NMR and  $^{31}\text{P}$ -NMR spectra. *Org Magn Reson* 17:88–91
- Kanamori K, Roberts JD (1983) A  $^{15}\text{N}$  NMR study of the barriers to isomerization about guanidinium and guanidino carbon nitrogen bonds in L-arginine. *J Am Chem Soc* 105:4698–4701
- Kanamori K, Cain AH, Roberts JD (1978) Studies of pH and anion complexation effects on L-arginine by natural abundance  $^{15}\text{N}$  nuclear magnetic resonance spectroscopy. *J Am Chem Soc* 100:4979–4981
- Kawano K, Kyogoku Y (1975) Nitrogen-15 nuclear magnetic-resonance of histidine—effect of pH. *Chem Lett* 12:1305–1308
- Kay LE (1993) Pulsed-field gradient-enhanced 3-dimensional NMR experiment for correlating  $^{13}\text{C}\alpha/\beta$ ,  $^{13}\text{C}^{\prime}$ , and  $^1\text{H}\alpha$  chemical-shifts in uniformly  $^{13}\text{C}$ -labeled proteins dissolved in  $\text{H}_2\text{O}$ . *J Am Chem Soc* 115:2055–2057
- Keim P, Vigna RA, Morrow JS, Marshall RC, Gurd FRN (1973)  $^{13}\text{C}$  nuclear magnetic-resonance of pentapeptides of glycine containing central residues of serine, threonine, aspartic and glutamic acids, asparagine, and glutamin. *J Biol Chem* 248:7811–7818
- Keim P, Vigna RA, Nigen AM, Morrow JS, Gurd FRN (1974)  $^{13}\text{C}$  nuclear magnetic-resonance of pentapeptides of glycine containing central residues of methionine, proline, arginine, and lysine. *J Biol Chem* 249:4149–4156
- Kesvatera T, Jonsson B, Thulin E, Linse S (1996) Measurement and modelling of sequence-specific pKa values of lysine residues in calbindin D9k. *J Mol Biol* 259:828–839
- Khare D, Alexander P, Antosiewicz J, Bryan P, Gilson M, Orban J (1997) pKa measurements from nuclear magnetic resonance for the B1 and B2 immunoglobulin G-binding domains of protein G: comparison with calculated values for nuclear magnetic resonance and X-ray structures. *Biochemistry* 36:3580–3589
- Kjaergaard M, Brander S, Poulsen FM (2011) Random coil chemical shift for intrinsically disordered proteins: effects of temperature and pH. *J Biomol NMR* 49:139–149
- Knowles JR (1976) The intrinsic pKa values of functional groups in enzymes: improper deductions from the pH-dependence of steady-state parameters. *CRC Crit Rev Biochem* 4:165–173
- Krezel A, Bal W (2004) A formula for correlating pKa values determined in  $\text{D}_2\text{O}$  and  $\text{H}_2\text{O}$ . *J Inorg Biochem* 98:161–166
- Kubickova A, Krizek T, Coufal P, Wernersson E, Heyda J, Jungwirth P (2011) Guanidinium cations pair with positively charged arginine side chains in water. *J Phys Chem Lett* 2:1387–1389
- Kucic P, Farrell D, Søndergaard CR, Bjarnadottir U, Bradley J, Pollastri G, Nielsen JE (2010) Improving the analysis of NMR spectra tracking pH-induced conformational changes: removing artefacts of the electric field on the NMR chemical shift. *Proteins Struct Func Bioinform* 78:971–984
- Kucic P et al (2013) Protein dielectric constants determined from NMR chemical shift perturbations. *J Am Chem Soc* 135:16968–16976
- Ladner HK, Led JJ, Grant DM (1975) Deuterium-isotope effects on  $^{13}\text{C}$  chemical shifts in amino acids and dipeptides. *J Magn Reson* 20:530–534
- Langkilde A et al (2008) Short strong hydrogen bonds in proteins: a case study of rhamnolacturonan acetyltransferase. *Acta Crystallogr D* 64:851–863
- Lau DKW, Okon M, McIntosh LP (2012) The PNT domain from *Drosophila* Pointed-P2 contains a dynamic N-terminal helix preceded by a disordered phosphoacceptor sequence. *Protein Sci* 21:1716–1725
- Lecomte C, Jelsch C, Guillot B, Fournier B, Lagoutte A (2008) Ultrahigh-resolution crystallography and related electron density and electrostatic properties in proteins. *J Synchrotron Rad* 15:202–203
- Led JJ, Petersen SB (1979) Deuterium-isotope effects on  $^{13}\text{C}$  chemical-shifts in selected amino-acids as function of pH. *J Magn Reson* 33:603–6170
- Legerton TL, Kanamori K, Weiss RL, Roberts JD (1981)  $^{15}\text{N}$  NMR studies of nitrogen metabolism in intact mycelia of *Neurospora crassa*. *Proc Natl Acad Sci* 78:1495–1498
- Li SH, Hong M (2011) Protonation, tautomerization, and rotameric structure of histidine: a comprehensive study by magic-angle-spinning solid-state NMR. *J Am Chem Soc* 133:1534–1544
- Licht S (1985) pH measurement in concentrated alkaline-solutions. *Anal Chem* 57:514–519
- Liepinsh E, Otting G (1996) Proton exchange rates from amino acid side chains—implications for image contrast. *Magn Reson Med* 35:30–42
- Liepinsh E, Otting G, Wüthrich K (1992) NMR spectroscopy of hydroxyl protons in aqueous solutions of peptides and proteins. *J Biomol NMR* 2:447–465
- Lim JC, Gruschus JM, Kim G, Berlett BS, Tjandra N, Levine RL (2012) A low pKa cysteine at the active site of mouse methionine sulfoxide reductase A. *J Biol Chem* 287:25596–25601
- Lindman S, Linse S, Mulder FA, Andre I (2006) Electrostatic contributions to residue-specific protonation equilibria and proton binding capacitance for a small protein. *Biochemistry* 45:13993–14002
- Lindman S, Linse S, Mulder FA, Andre I (2007) pKa values for side-chain carboxyl groups of a PGB1 variant explain salt and pH-dependent stability. *Biophys J* 92:257–266
- Löhr F, Katsemi V, Betz M, Hartleib J, Rüterjans H (2002) Sequence-specific assignment of histidine and tryptophan ring  $^1\text{H}$ ,  $^{13}\text{C}$  and  $^{15}\text{N}$  resonances in  $^{13}\text{C}/^{15}\text{N}$ - and  $^2\text{H}/^{13}\text{C}/^{15}\text{N}$ -labelled proteins. *J Biomol NMR* 22:153–164
- Löhr F, Rogov VV, Shi MC, Bernhard F, Dötsch V (2005) Triple-resonance methods for complete resonance assignment of aromatic protons and directly bound heteronuclei in histidine and tryptophan residues. *J Biomol NMR* 32:309–328
- London RE (1980) Correlation of carboxyl carbon titration shifts and pK values. *J Magn Reson* 38:173–177

- London RE, Walker TE, Whaley TW, Matwiyoff NA (1977)  $^{15}\text{N}$  NMR studies of  $^{13}\text{C}$ ,  $^{15}\text{N}$  labeled arginine. *Org Magn Reson* 9:598–600
- London RE, Walker TE, Kollman VH, Matwiyoff NA (1978) Studies of pH-dependence of  $^{13}\text{C}$  shifts and carbon-carbon coupling-constants of  $[\text{U-}^{13}\text{C}]$ aspartic and glutamic acids. *J Am Chem Soc* 100:3723–3729
- Ludwiczek ML et al (2013) Strategies for modulating the pH-dependent activity of a family 11 glycoside hydrolase. *Biochemistry* 52:3138–3156
- Markley JL (1975) Observation of histidine residues in proteins by means of nuclear magnetic-resonance spectroscopy. *Acc Chem Res* 8:70–80
- Mavridou DAI, Stevens JM, Ferguson SJ, Redfield C (2007) Active-site properties of the oxidized and reduced C-terminal domain of DsbD obtained by NMR spectroscopy. *J Mol Biol* 370:643–658
- Mayer R, Lancelot G, Spach G (1979) Side chain-backbone hydrogen-bonds in peptides containing glutamic-acid residues. *Biopolymers* 18:1293–1296
- McIntosh LP, Wand AJ, Lowry DF, Redfield AG, Dahlquist FW (1990) Assignment of the backbone  $^1\text{H}$  and  $^{15}\text{N}$  NMR resonances of bacteriophage T4 lysozyme. *Biochemistry* 29:6341–6362
- McIntosh LP et al (1996) The pKa of the general acid/base carboxyl group of a glycosidase cycles during catalysis: a  $^{13}\text{C}$ -NMR study of *Bacillus circulans* xylanase. *Biochemistry* 35:9958–9966
- McIntosh LP, Kang HS, Okon M, Nelson ML, Graves BJ, Brutscher B (2009) Detection and assignment of phosphoserine and phosphothreonine residues by  $^{13}\text{C}$ - $^{31}\text{P}$  spin-echo difference NMR spectroscopy. *J Biomol NMR* 43:31–37
- McIntosh LP, Naito D, Baturin SJ, Okon M, Joshi MD, Nielsen JE (2011) Dissecting electrostatic interactions in *Bacillus circulans* xylanase through NMR-monitored pH titrations. *J Biomol NMR* 51:5–19
- McMahon BH et al (2004) FTIR studies of internal proton transfer reactions linked to inter-heme electron transfer in bovine cytochrome c oxidase. *Biochim Biophys Acta* 1655:321–331
- Miao Y, Cross TA, Fu R (2014) Differentiation of histidine tautomeric states using  $^{15}\text{N}$  selectively filtered  $^{13}\text{C}$  solid-state NMR spectroscopy. *J Magn Reson* 245C:105–109
- Mossner E, Iwai H, Glockshuber R (2000) Influence of the pKa value of the buried, active-site cysteine on the redox properties of thioredoxin-like oxidoreductases. *FEBS Lett* 477:21–26
- Munowitz M, Bachovchin WW, Herzfeld J, Dobson CM, Griffin RG (1982) Acid-base and tautomeric equilibria in the solid-state— $^{15}\text{N}$  NMR spectroscopy of histidine and imidazole. *J Am Chem Soc* 104:1192–1196
- Nielsen JE, Gunner MR, Garcia-Moreno BE (2011) The pKa Cooperative: a collaborative effort to advance structure-based calculations of pKa values and electrostatic effects in proteins. *Proteins* 79:3249–3259
- Niimura N, Bau R (2008) Neutron protein crystallography: beyond the folding structure of biological macromolecules. *Acta Cryst Section A* 64:12–22
- Norberg J, Foloppe N, Nilsson L (2005) Intrinsic relative stabilities of the neutral tautomers of arginine side-chain models. *J Chem Theory Comput* 1:986–993
- Nordstrand K, Aslund F, Meunier S, Holmgren A, Otting G, Berndt KD (1999) Direct NMR observation of the Cys-14 thiol proton of reduced *Escherichia coli* glutaredoxin-3 supports the presence of an active site thiol-thiolate hydrogen bond. *FEBS Lett* 449:196–200
- Norton RS, Bradbury JH (1974)  $^{13}\text{C}$  nuclear magnetic-resonance study of tyrosine titrations. *J Chem Soc Chem Comm* 21:870–871
- Oda Y, Yamazaki T, Nagayama K, Kanaya S, Kuroda Y, Nakamura H (1994) Individual ionization-constants of all the carboxyl groups in ribonuclease HI from *Escherichia coli* determined by NMR. *Biochemistry* 33:5275–5284
- Oktaviani NA, Pool TJ, Kamikubo H, Slager J, Scheek RM, Kataoka M, Mulder FAA (2012) Comprehensive determination of protein tyrosine pKa values for photoactive yellow protein using indirect  $^{13}\text{C}$  NMR spectroscopy. *Biophys J* 102:579–586
- Oldfield E, Norton RS, Allerhand A (1975a) Studies of individual carbon sites of proteins in solution by natural abundance carbon 13 nuclear magnetic-resonance spectroscopy—relaxation behavior. *J Biol Chem* 250:6368–6380
- Oldfield E, Norton RS, Allerhand A (1975b) Studies of individual carbon sites of proteins in solution by natural abundance carbon 13 nuclear magnetic-resonance spectroscopy—strategies for assignments. *J Biol Chem* 250:6381–6402
- Parsons SM, Raftery MA (1972) Ionization behavior of the catalytic carboxyls of lysozyme. Effects of ionic strength. *Biochemistry* 11:1623–1629
- Pellecchia M, Wider G, Iwai H, Wüthrich K (1997) Arginine side chain assignments in uniformly  $^{15}\text{N}$ -labeled proteins using the novel 2D  $\text{H}\epsilon(\text{N}\epsilon)\text{H}\gamma\text{HH}$  experiment. *J Biomol NMR* 10:193–197
- Pelton JG, Torchia DA, Meadow ND, Roseman S (1993) Tautomeric states of the active-site histidines of phosphorylated and unphosphorylated III(Glc), a signal-transducing protein from *Escherichia coli*, using 2-dimensional heteronuclear NMR techniques. *Protein Sci* 2:543–558
- Petkova AT, Hu JG, Bizounok M, Simpson M, Griffin RG, Herzfeld J (1999) Arginine activity in the proton-motive photocycle of bacteriorhodopsin: solid-state NMR studies of the wild-type and D85N proteins. *Biochemistry* 38:1562–1572
- Plesniak LA, Connelly GP, Wakarchuk WW, McIntosh LP (1996) Characterization of a buried neutral histidine residue in *Bacillus circulans* xylanase: NMR assignments, pH titration, and hydrogen exchange. *Protein Sci* 5:2319–2328
- Poon DKY, Schubert M, Au J, Okon M, Withers SG, McIntosh LP (2006) Unambiguous determination of the ionization state of a glycoside hydrolase active site lysine by  $^1\text{H}$ - $^{15}\text{N}$  heteronuclear correlation spectroscopy. *J Am Chem Soc* 128:15388–15389
- Popov K, Ronkkomaki H, Lajunen LHJ (2006) Guidelines for NMR measurements for determination of high and low pKa values. *Pure Appl Chem* 78:663–675
- Pregosin PS, Randall EW, White AI (1971) Natural abundance  $^{15}\text{N}$  nuclear magnetic resonance spectroscopy—amino acid derivatives. *J Chem Soc Chem Comm* 24:1602–1603
- Prestegard JH, Sahu SC, Nkari WK, Morris LC, Live D, Gruta C (2013) Chemical shift prediction for denatured proteins. *J Biomol NMR* 55:201–209
- Prompers JJ, Groenewegen A, Hilbers CW, Pepermans HAM (1998) Two-dimensional NMR experiments for the assignment of aromatic side chains in  $^{13}\text{C}$ -labeled proteins. *J Magn Reson* 130:68–75
- Pujato M, Navarro A, Versace R, Mancusso R, Ghose R, Tasayco ML (2006) The pH-dependence of amide chemical shift of Asp/Glu reflects its pKa in intrinsically disordered proteins with only local interactions. *BBA-Proteins Proteom* 1764:1227–1233
- Quirt AR, Lyerla JR, Peat IR, Cohen JS, Reynolds WF, Freedman MH (1974)  $^{13}\text{C}$  nuclear magnetic resonance titration shifts in amino-acids. *J Am Chem Soc* 96:570–571
- Rabenstein DL, Sayer TL (1976a)  $^{13}\text{C}$  chemical shift parameters for amines, carboxylic acids, and amino acids. *J Magn Reson* 24:27–39
- Rabenstein DL, Sayer TL (1976b) Determination of microscopic acid dissociation constants by nuclear magnetic-resonance spectrometry. *Anal Chem* 48:1141–1145
- Raczynska ED et al (2003) Consequences of proton transfer in guanidine. *J Phys Org Chem* 16:91–106
- Rajagopal P, Waygood EB, Klevit RE (1994) Structural consequences of histidine phosphorylation—NMR characterization of the phosphohistidine form of histidine-containing protein from *Bacillus subtilis* and *Escherichia coli*. *Biochemistry* 33:15271–15282

- Rao NS, Legault P, Muhandiram DR, Greenblatt J, Battiste JL, Williamson JR, Kay LE (1996) NMR pulse schemes for the sequential assignment of arginine side-chain H $\alpha$  protons. *J Magn Reson Ser B* 113:272–276
- Reynolds WF, Tzeng CW (1977) Determination of preferred tautomeric form of histamine by  $^{13}\text{C}$  NMR spectroscopy. *Can J Biochem Cell B* 55:576–578
- Reynolds WF, Peat IR, Freedman MH, Lyerla JR Jr (1973) Determination of the tautomeric form of the imidazole ring of L-histidine in basic solution by  $^{13}\text{C}$  magnetic resonance spectroscopy. *J Am Chem Soc* 95:328–331
- Richards RE, Thomas NA (1974) Nitrogen-14 nuclear magnetic-resonance study of amino acids, peptides, and other biologically interesting molecules. *J Chem Soc Perk T* 2:368–374
- Richarz R, Wüthrich K (1978)  $^{13}\text{C}$  NMR chemical-shifts of common amino acid residues measured in aqueous-solutions of linear tetrapeptides H-Gly-Gly-X-L-Ala-OH. *Biopolymers* 17:2133–2141
- Roberts JD, Yu C, Flanagan C, Birdseye TR (1982) A  $^{15}\text{N}$  nuclear magnetic-resonance study of the acid-base and tautomeric equilibria of 4-substituted imidazoles and its relevance to the catalytic mechanism of  $\alpha$ -lytic protease. *J Am Chem Soc* 104:3945–3949
- Robillard G, Shulman RG (1972) High-resolution nuclear magnetic-resonance study of histidine—aspartate hydrogen-bond in chymotrypsin and chymotrypsinogen. *J Mol Biol* 71:507–511
- Roos G, Foloppe N, Messens J (2013) Understanding the pKa of redox cysteines: the key role of hydrogen bonding. *Antioxid Redox Sign* 18:94–127
- Saito K, Ishikita H (2012) H atom positions and nuclear magnetic resonance chemical shifts of short H bonds in photoactive yellow protein. *Biochemistry* 51:1171–1177
- Sattler M, Schleucher J, Griesinger C (1999) Heteronuclear multidimensional NMR experiments for the structure determination of proteins in solution employing pulsed field gradients. *Prog Nucl Mag Reson Specty* 34:93–158
- Schaller W, Robertson AD (1995) pH, ionic strength, and temperature dependences of ionization equilibria for the carboxyl groups in turkey ovomucoid third domain. *Biochemistry* 34:4714–4723
- Schlemmer H, Sontheimer GM, Kalbitzer HR (1988)  $^{31}\text{P}$  nuclear magnetic-resonance spectroscopy of the phosphorylated tetrapeptide Gly-Gly-Asp-Ala. *Magn Reson Chem* 26:260–263
- Schlippe YVG, Hedstrom L (2005) A twisted base? The role of arginine in enzyme-catalyzed proton abstractions. *Arch Biochem Biophys* 433:266–278
- Schubert M et al (2007) Probing electrostatic interactions along the reaction pathway of a glycoside hydrolase: histidine characterization by NMR spectroscopy. *Biochemistry* 46:7383–7395
- Schwarzinger S, Kroon GJA, Foss TR, Chung J, Wright PE, Dyson HJ (2001) Sequence-dependent correction of random coil NMR chemical shifts. *J Am Chem Soc* 123:2970–2978
- Segawa T, Kateb F, Duma L, Bodenhausen G, Pelulessy P (2008) Exchange rate constants of invisible protons in proteins determined by NMR spectroscopy. *ChemBioChem* 9:537–542
- Shimba N, Takahashi H, Sakakura M, Fujii I, Shimada I (1998) Determination of protonation and deprotonation forms and tautomeric states of histidine residues in large proteins using nitrogen-carbon J couplings in imidazole ring. *J Am Chem Soc* 120:10988–10989
- Shrager RI, Sachs DH, Schechte A, Cohen JS, Heller SR (1972) Nuclear magnetic-resonance titration curves of histidine ring protons. 2. Mathematical models for interacting groups in nuclear magnetic-resonance titration curves. *Biochemistry* 11:541–547
- Smet-Nocca C, Launay H, Wieruszkeski JM, Lippens G, Landrieu I (2013) Unraveling a phosphorylation event in a folded protein by NMR spectroscopy: phosphorylation of the Pin1 WW domain by PKA. *J Biomol NMR* 55:323–337
- Smith BC, Denu JM (2009) Chemical mechanisms of histone lysine and arginine modifications. *BBA-Gene Regul Mech* 1789:45–57
- Smith GM, Yu LP, Domingues DJ (1987) Directly observed  $^{15}\text{N}$  NMR spectra of uniformly enriched proteins. *Biochemistry* 26:2202–2207
- Søndergaard CR, McIntosh LP, Pollastri G, Nielsen JE (2008) Determination of electrostatic interaction energies and protonation state populations in enzyme active sites. *J Mol Biol* 376:269–287
- Song JK, Laskowski M, Qasim MA, Markley JL (2003) NMR determination of pKa values for Asp, Glu, His, and Lys mutants at each variable contiguous enzyme-inhibitor contact position of the turkey ovomucoid third domain. *Biochemistry* 42:2847–2856
- Spitzner N, Löhner F, Pfeiffer S, Koumanov A, Karshikoff A, Rüterjans H (2001) Ionization properties of titratable groups in ribonuclease T1—I. pKa values in the native state determined by two-dimensional heteronuclear NMR spectroscopy. *Eur Biophys J* with s 30:186–197
- Sudmeier JL, Ash EL, Gunther UL, Luo XL, Bullock PA, Bachovchin WW (1996) HCN, a triple-resonance NMR technique for selective observation of histidine and tryptophan side chains in  $^{13}\text{C}/^{15}\text{N}$ -labeled proteins. *J Magn Reson Ser B* 113:236–247
- Sudmeier JL, Bradshaw EM, Haddad KE, Day RM, Thalhauser CJ, Bullock PA, Bachovchin WW (2003) Identification of histidine tautomers in proteins by 2D  $^1\text{H}/^{13}\text{C}^{\text{O}2}$  one-bond correlated NMR. *J Am Chem Soc* 125:8430–8431
- Surprenant HL, Sarneski JE, Key RR, Byrd JT, Reilly CN (1980)  $^{13}\text{C}$  NMR studies of amino acids—chemical-shifts, protonation shifts, microscopic protonation behavior. *J Magn Reson* 40:231–243
- Suzuki T, Yamaguchi T, Imanari M (1974)  $^{15}\text{N}$  FT NMR spectra of amino acids in natural abundance—pH-dependence of  $^{15}\text{N}$  chemical-shifts for L-arginine. *Tetrahedron Lett* 20:1809–1812
- Szakacs Z, Kraszni M, Noszal B (2004) Determination of microscopic acid-base parameters from NMR pH titrations. *Anal Bioanal Chem* 378:1428–1448
- Takayama Y, Castaneda CA, Chimenti M, Garcia-Moreno B, Iwahara J (2008a) Direct evidence for deprotonation of a lysine side chain buried in the hydrophobic core of a protein. *J Am Chem Soc* 130:6714–6715
- Takayama Y, Sahu D, Iwahara J (2008b) Observing in-phase single-quantum  $^{15}\text{N}$  multiplets for  $\text{NH}_2/\text{NH}_3^+$  groups with two-dimensional heteronuclear correlation spectroscopy. *J Magn Reson* 194:313–316
- Takeda M, Jee J, Ono AM, Terauchi T, Kainosho M (2009) Hydrogen exchange rate of tyrosine hydroxyl groups in proteins as studied by the deuterium isotope effect on  $\text{C}^5$  chemical shifts. *J Am Chem Soc* 131:18556–18562
- Takeda M, Jee J, Terauchi T, Kainosho M (2010) Detection of the sulfhydryl groups in proteins with slow hydrogen exchange rates and determination of their proton/deuteron fractionation factors using the deuterium-induced effects on the  $^{13}\text{C}^{\beta}$  NMR signals. *J Am Chem Soc* 132:6254–6260
- Takeda M, Miyanoiri Y, Terauchi T, Yang C-J, Kainosho M (2014) Use of H/D isotope effects to gather information about hydrogen bonding and hydrogen exchange rates. *J Magn Reson* 241:148–154
- Tamiola K, Acar B, Mulder FAA (2010) Sequence-specific random coil chemical shifts of intrinsically disordered proteins. *J Am Chem Soc* 132:18000–18003
- Tanokura M (1983)  $^1\text{H}$ -NMR study on the tautomerism of the imidazole ring of histidine-residues 1. Microscopic pK values and molar ratios of tautomers in histidine-containing peptides. *Biochim Biophys Acta* 742:576–585
- Thanabal V, Omecinsky DO, Reilly MD, Cody WL (1994) The  $^{13}\text{C}$  chemical shifts of amino acids in aqueous-solution containing organic-solvents—application to the secondary structure characterization of peptides in aqueous trifluoroethanol solution. *J Biomol NMR* 4:47–59

- Theillet FX et al (2012) Cell signaling, post-translational protein modifications and NMR spectroscopy. *J Biomol NMR* 54:217–236
- Tolbert BS, Tajc SG, Webb H, Snyder J, Nielsen JE, Miller BL, Basavappa R (2005) The active site cysteine of ubiquitin-conjugating enzymes has a significantly elevated pKa: functional implications. *Biochemistry* 44:16385–16391
- Tolstoy PM, Schah-Mohammadi P, Smirnov SN, Golubev NS, Denisov GS, Limbach HH (2004) Characterization of fluxional hydrogen-bonded complexes of acetic acid and acetate by NMR: geometries and isotope and solvent effects. *J Am Chem Soc* 126:5621–5634
- Tomlinson JH, Ullah S, Hansen PE, Williamson MP (2009) Characterization of salt bridges to lysines in the protein G B1 domain. *J Am Chem Soc* 131:4674–4684
- Tomlinson JH, Green VL, Baker PJ, Williamson MP (2010) Structural origins of pH-dependent chemical shifts in the B1 domain of protein G. *Proteins Struct Funct Bioinform* 78:3000–3016
- Tugarinov V (2014) Indirect use of deuterium in solution NMR studies of protein structure and hydrogen bonding. *Prog Nucl Magn Reson Spectr* 77:49–68
- Ullah S, Ishimoto T, Williamson MP, Hansen PE (2011) Ab initio calculations of deuterium isotope effects on chemical shifts of salt-bridged lysines. *J Phys Chem B* 115:3208–3215
- Ullmann GM (2003) Relations between protonation constants and titration curves in polyprotic acids: a critical view. *J Phys Chem B* 107:1263–1271
- Ulrich EL et al (2008) BioMagResBank. *Nucleic Acids Res* 36:D402–D408
- van Dijk AA, Delange LCM, Bachovchin WW, Robillard GT (1990) Effect of phosphorylation on hydrogen-bonding interactions of the active-site histidine of the phosphocarrier protein hpr of the phosphoenolpyruvate-dependent phosphotransferase system determined by  $^{15}\text{N}$  NMR spectroscopy. *Biochemistry* 29:8164–8171
- Velyvis A, Kay LE (2013) Measurement of active site ionization equilibria in the 670 kDa proteasome core particle using methyl-TROSY NMR. *J Am Chem Soc* 135:9259–9262
- Vis H, Boelens R, Mariani M, Stroop R, Vorgias CE, Wilson KS, Kaptein R (1994)  $^1\text{H}$ ,  $^{13}\text{C}$ , and  $^{15}\text{N}$  resonance assignments and secondary structure-analysis of the hu protein from *Bacillus stearothermophilus* using 2-dimensional and 3-dimensional double-resonance and triple-resonance heteronuclear magnetic-resonance spectroscopy. *Biochemistry* 33:14858–14870
- Volpon L et al (2007) NMR structure determination of a synthetic analogue of bacillomycin Lc reveals the strategic role of L-Asn1 in the natural iturinic antibiotics. *Spectrochim Acta Part A* 67:1374–1381
- Vondrasek J, Mason PE, Heyda J, Collins KD, Jungwirth P (2009) The molecular origin of like-charge arginine-arginine pairing in water. *J Phys Chem B* 113:9041–9045
- Wang YJ, Jardetzky O (2002) Investigation of the neighboring residue effects on protein chemical shifts. *J Am Chem Soc* 124:14075–14084
- Wang YX et al (1996) Solution NMR evidence that the HIV-1 protease catalytic aspartyl groups have different ionization states in the complex formed with the asymmetric drug KNI-272. *Biochemistry* 35:9945–9950
- Wasylishen RE, Friedrich JO (1987) Deuterium-isotope effects on nuclear shielding constants and spin spin coupling-constants in the ammonium ion, ammonia, and water. *Can J Chem* 65:2238–2243
- Wasylishen RE, Tomlinson G (1975) pH-dependence of  $^{13}\text{C}$  chemical-shifts and  $^{13}\text{C}$ , H coupling-constants in imidazole and L-histidine. *Biochem J* 147:605–607
- Wasylishen RE, Tomlinson G (1977) Applications of long-range  $^{13}\text{C}$ , H nuclear spin-spin coupling-constants in study of imidazole tautomerism in L-histidine, histamine, and related compounds. *Can J Biochem Cell B* 55:579–582
- Webb H, Tynan-Connolly BM, Lee GM, Farrell D, O'Meara F, Søndergaard CR, Teilmann K, Hewage C, McIntosh LP, Nielsen JE (2011) Remeasuring HEWL pKa values by NMR spectroscopy: methods, analysis, accuracy, and implications for theoretical pKa, calculations. *Proteins Struct Funct Bioinform* 79:685–702
- Werner MH, Clore GM, Fisher CL, Fisher RJ, Trinh L, Shiloach J, Gronenborn AM (1997) Correction of the NMR structure of the ETS1/DNA complex. *J Biomol NMR* 10:317–328
- Wilson NA, Barbar E, Fuchs JA, Woodward C (1995) Aspartic-acid 26 in reduced escherichia-coli thioredoxin has a pKa(a) >9. *Biochemistry* 34:8931–8939
- Wishart DS (2011) Interpreting protein chemical shift data. *Prog Nucl Magn Reson Spectr* 58:62–87
- Wishart DS, Bigam CG, Holm A, Hodges RS, Sykes BD (1995)  $^1\text{H}$ ,  $^{13}\text{C}$  and  $^{15}\text{N}$  random coil NMR chemical-shifts of the common amino-acids 1. Investigations of nearest-neighbor effects. *J Biomol NMR* 5:67–81
- Witanowski M, Webb GA, Stefania L, Januszew H, Grabowski Z (1972) Nitrogen-14 nuclear magnetic resonance of azoles and their benzo derivatives. *Tetrahedron* 28:637–653
- Witanowski M, Stefaniak L, Szymanski S, Webb GA (1976)  $^{14}\text{N}$  NMR study of isomeric structures of urea and its analogs. *Tetrahedron* 32:2127–2129
- Wittekind M, Metzler WJ, Mueller L (1993) Selective correlations of amide groups to glycine alpha-protons in proteins. *J Magn Reson Ser B* 101:214–217
- Wu XJ, Westler WM, Markley JL (1984) The assignment of imidazolium  $\text{N}^{\text{H}}\text{-H}^1$  peaks in the  $^1\text{H}$ -NMR spectrum of a protein by one-dimensional and two-dimensional NOE experiments. *J Magn Reson* 59:524–529
- Wüthrich K, Wagner G (1979) Nuclear magnetic-resonance of labile protons in the basic pancreatic trypsin-inhibitor. *J Mol Biol* 130:1–18
- Xiao YW, Braiman M (2005) Modeling amino acid side chains in proteins:  $^{15}\text{N}$  NMR spectra of guanidino groups in nonpolar environments. *J Phys Chem B* 109:16953–16958
- Xiao Y, Hutson MS, Belenky M, Herzfeld J, Braiman MS (2004) Role of arginine-82 in fast proton release during the bacteriorhodopsin photocycle: a time-resolved FT-IR study of purple membranes containing  $^{15}\text{N}$ -labeled arginine. *Biochemistry* 43:12809–12818
- Yamazaki T, Yoshida M, Nagayama K (1993) Complete assignments of magnetic resonances of ribonuclease-H from *Escherichia coli* by double-resonance and triple-resonance 2D and 3D NMR spectroscopies. *Biochemistry* 32:5656–5669
- Yamazaki T et al (1994) NMR and X-ray evidence that the HIV protease catalytic aspartyl groups are protonated in the complex formed by the protease and a nonpeptide cyclic urea-based inhibitor. *J Am Chem Soc* 116:10791–10792
- Yamazaki T, Pascal SM, Singer AU, Forman-Kay JD, Kay LE (1995) NMR pulse schemes for the sequence-specific assignment of arginine guanidino  $^{15}\text{N}$  and  $^1\text{H}$  chemical-shifts in proteins. *J Am Chem Soc* 117:3556–3564
- Yavari I, Roberts JD (1978) Differential rates of proton-exchange for guanidinium nitrogens of L-arginine determined by natural-abundance  $^{15}\text{N}$  nuclear magnetic-resonance spectroscopy. *Biochem Biophys Res Commun* 83:635–640
- Yu LP, Fesik SW (1994) pH titration of the histidine-residues of cyclophilin and FK506 binding-protein in the absence and presence of immunosuppressant ligands. *Bioc Biophys Acta Prot Struct Molr Enzym* 1209:24–32
- Zandarashvili L, Li DW, Wang T, Bruschweiler R, Iwahara J (2011) Signature of mobile hydrogen bonding of lysine side chains from long-range  $^{15}\text{N}$ - $^{13}\text{C}$  scalar J-couplings and computation. *J Am Chem Soc* 133:9192–9195

Zandarashvili L, Esadze A, Iwahara J (2013) NMR Studies on the dynamics of hydrogen bonds and ion pairs involving lysine side chains of proteins. *Adv Protein Chem Str* 93:37–80

Zheng G, Price WS (2010) Solvent signal suppression in NMR. *Prog Nuclear Magn Res Spect* 56:267–288

Zhu L, Kemple MD, Yuan P, Prendergast FG (1995) N-terminus and lysine side chain pKa values of melittin in aqueous solutions and micellar dispersions measured by  $^{15}\text{N}$  NMR. *Biochemistry* 34:13196–13202